The University of Nottingham

UNITED KINGDOM · CHINA · MALAYSIA

Tailoring the Structure of Nanomaterials Formed by Light-Induced Synthesis

by Vladimir Astachov

Thesis submitted to the University of Nottingham
for the Degree of Doctor of Philosophy

Main Supervisor: Prof. Andrew Long

Second Supervisor: Prof. Derek Irvine

January 2018

Table of Contents

Abstract

A light is an energy portion that plays a very important role in nature. A light particle or photon can be absorbed, scattered or reflected. In some cases, light can greatly influence the formation of a crystal and guide its growth into hierarchical nano or microstructure.

This work explores the light-induced synthesis of nanomaterials (Au, Ag, CdS, ZnO) and light-induced polymer nanostructuration. This way of synthesizing nanomaterials is compared to other known routes. The main advantage of the synthesis method presented here is its ability to be used for water-based reactions at room temperature. This method can be applied to most water-based syntheses. In this work, results have been compared with template-assisted synthesis for Ag, CdS, and Au. The ZnO light-induced synthesis was used and compared to the hydrothermal ZnO synthesis method.

First, the effect of light over the synthesis of ZnO, Ag and semiconducting polymer P3HT and its mixture with $PC_{[70]}BM$ is demonstrated. The main results from this work include that computer-assisted light control systems might provide a shape-selective synthesis of nano/microstructures at room temperature. Also, light-assisted synthesis provides crystal growth without the use of a capping agent or polymer template.

Morphology control of polymer-monomer mixture is demonstrated which was achieved using Red and Blue LEDs. It was found that Red light increased the diameter of the voids in polymer films while on the contrary blue light decreased it. For ease of comparison, the mixed solvent study was carried out on the same polymers. The change of electrostatic interaction reflected on the change of the morphology of the polymer films. Templated Ag nanostructure synthesis was also performed showing different results when in the presence of light structures are more uniform and have

higher surface area. The work also demonstrates template-assisted synthesis of CdS quantum dots. The use of PPI type dendrimer showed that self-assembly of CdS quantum dots in a nanofiber is achievable at room temperature. Au nanostructures were synthesized using another organic template oleic acid. Synthesis results showed unusual Au nanoparticle morphologies.

Finally, low-power light was shown to influence the nanostructure synthesis and structuration at room temperature. The main effect was the change in the shape due to the vibration of water molecules. Water absorbs light mostly on the infrared region and very little in the visible range. Due to the low absorbance of visible light by water, it required longer time intervals in order to achieve the changes in morphology of the ZnO or Ag structures. Reaction time has been proven to be an important factor in light-matter interaction. In this work, AFM, SEM, UV-vis, PL, NMR and TEM were used for the characterisation of materials synthesized at room temperature.

Acknowledgements

I am deeply grateful to Professor Andrew Long for his support, supervision and guidance. Also thanks to Professor Derek Irvine for the useful suggestions in chemistry and supervision. I would also like to thank Professor Amir Fahmi for his supervision during my first year and for his help both in physics and chemistry. I would like to thank Professor Kwang Leong Choy for her supervision during my second year and for the support and guidance. I am very thankful to Professor advice in chemistry and support.

Special thanks to Professor for his support and guidance during my work in the Nanomaterials laboratory. I am grateful to all my friends in England, Lithuania and in the rest of the World.

I am especially grateful to my special friends in Nottingham. J J J

And I am above all thankful to my parents and dedicate this work to them.

And of course...I am thankful to all the scientists in the World throughout history that never gave up on their science!!!

Abbreviations

AFM- Atomic Force Microscope

CB- Chlorobenzene

CHF- Chloroform

CTAC- Cetyltrimethylammonium chloride

DMF ï Dimethylformamide

Dpm- particle density

EDX- Energy-dispersive X-ray Spectroscopy

EG-ethylene glycol

ESEM- Environmental Scanning Electron Microscope

FFT- Fast Fourier Transform

HRTEM- High-Resolution Transmission Electron Microscopy

HAADF- High Angle Annular Dark Field (imaging)

LED- Light Emmiting Diode

NMR- Nuclear Magnetic Resonance

NP- nanoparticle

PAMAM- polyamido amines (dendrimers)

PCE-Power Conversion Efficiency

PEG- polyethylene glycol

PPI-G4- polypropylene ymine dendrimer generation 4

$PC_{[70]}BM$ - Phenyl-Butyric-Acid-Methyl Ester with fullerene 60 or 70

P3HT ï Poly-3 hexylthiophene 2.5 dyil regioregular.

PL ï Photoluminescence

PTB7- Poly({4,8-bis[(2-ethylhexyl)oxy]benzo[1,2-b:4,5-b Nj] d i t -2,6-diyl}{3-fluoro-2-[(2-ethylhexyl)carbonyl]thieno[3,4-b]thiophenediyl})

PVP- Polyvinylpyrrolidone

STEM- Scanning Transmission Electron Microscopy

QD- quantum dots

THF- Tetrahydrofuran

TEM- Transmission Electron Microscopy

UV-vis ï Utraviolet visible

Chapter 1 Introduction

The most problematic questions today are those related to energy [1] and pollution [2, 3] and are technology challenges which drive the whole science-community to create and promote solutions in order to address them. Nanoscience is providing goods and solutions for almost any problem starting from clean water [4] to medicine [5, 6]. Nanotechnology became very popular over the last few decades and offers a great future to humankind. Nanorobots in the future should be able to solve serious problems like starvation, diagnosis problems in medicine, space etc. [7, 8]. Recently nanostructurized silicon-based solar cell achieved 22% efficiency [9] and research increases in this area. Nanoscience brings novelties to society by improving devices and thus helping to improve our lives. However, the nanostructures synthesis procedure is specific for every material and morphology [10ï 14]. Tunnelling microscopes are able to build structures atom by atom which allows to build nanometer-sized objects but does enable mass production because it is time-consuming and expensive [15]. Nanomaterials depending on their size and shape possess different physical and chemical properties [16ï 20]. The synthesis of defined and/or complicated shapes was always a challenge [21ï 23]. The synthesis of nanomaterials usually requires toxic chemicals, also elevated temperatures are used in nanomaterial synthesis [24, 25]. Photochemical synthesis methods are limited in materials (Ag and photoreactive chemicals) and usually ultraviolet (UV) light is used which has a high energy in comparison to visible light [26ï 29]. The investigation of the formation of nanoparticles and other nano and microstructures was also poorly described by researchers [24ï 29]. Photochemical synthesis allows the use of less toxic materials and room temperature is usually enough for the reaction. On the other hand, control over the synthesis becomes difficult due to the limited variation ability during the synthesis. This is why existing experimental methods need to be upgraded which might be achieved if the hybrid method will be proposed (photochemical-sol-gel for instance). Improving nanochemical synthesis methods would upgrade the whole nanochemistry and other related disciplines as well. The main problem in synthesis of nanosized structures is that it is not possible to change the synthesis conditions at a certain point of synthesis time. If there is a template synthesis, then the chemicals dissolved in the solution sometimes cannot be suddenly removed if required. If there

is a synthesis at elevated temperature, then the solution cannot be cooled down immediately which sometimes could stop the reaction and leave the desired shape of metal nanoparticles. To overcome these problems a more flexible synthesis method is required. Photochemical or light-induced synthesis allows such changes during the synthesis. The light wavelength can be changed at any moment of the synthesis and the time of the irradiation can also be changed as desired. Also, elevated temperature is not necessary for the light-induced synthesis. The reaction can be stopped at any moment preventing the nanostructures from further growth. On the contrary, light-assisted synthesis also needs to be improved and upgraded.

1.1 Aims

The main aim of this work is to demonstrate the controlled synthesis and nano/micro structuration conception with Ag, Au, Ag-Au, ZnO, CdS, P3HT/ $PC_{[70]}BM$. This proposed method is different from the already existing methods since it it cheaper and more efficient. In the case of light-induced synthesis, it combines several wavelengths of light in one synthesis chamber. The method set-up allows the control of the time interval within irradiation period. The key project aim is to put light-induced conception along with other well know popular synthesis methods and use. And importantly to understand the light-matter interaction on the nanoscale in order to grow a variety of hierarchical nanostructures. This method solves the synthesis flexibility problems mentioned on the previous page (Ch.1 Introduction).

1.2 Major Work C onducted

To achieve the aims in 1.1 the main work steps have been proposed as follows:

- To synthesize ZnO and Ag hierarchical nanostructures under the Light Emitting Diode (LED) light, and to tailor the morphology of the polymer films using the same experimental set-up. Experiments in dark without the use of LED light will be conducted to study the influence of light irradiation. Conventional hydrothermal and template-assisted synthesis methods will also be carried out for comparison.
- To characterize ZnO, Au and Ag nanostructures using the scanning electron microscope. And to use the atomic force microscope for topographical characterization of polymer films.

- To assess the experimental results with existing theories that can explain the formation of the nanostructures and light-induced synthesis. And to evaluate the influence of light on the formation of the nanostructures.
- To study the mechanism on the light influence on the growth of the crystal structures. A nanostructure growth model will be established.
- The advantages and disadvantages of light-induced synthesis over known traditional synthesis methods will be highlighted, and research direction for future work will be proposed.

1.3 Outline of T hesis

The present work consists of seven chapters. Chapter 2 reviews popular nanomaterial synthesis methods and routes such as vapour-liquid-solid synthesis (VLS), Sol-gel, Hydrothermal, Photochemical, and Template-assisted. Also, the role of nanomorphology of most popular semiconducting polymer films used in nanoscience was reviewed and analysed.

Chapter 3 describes the experimental methodology in detail. Starting from the raw chemicals used and ending with the equipment used for the characterization. Specifics of each experiment are highlighted and sample preparations for every characterization are described in detail. Schematic depictions of most complicated experiments are included in the chapter with descriptions in order to make the experiments repeatable for the reader with minimum skills.

Chapter 4 focuses on polymer film morphology change and characterization using Atomic Force Microscope and Nuclear Magnetic Resonance. Polymer morphologies are analyzed and influence of solvents and light are discussed in detail.

Chapter 5 covers the template-assisted synthesis of Au and CdS. For the synthesis of Au oleic acid was chosen as a template to drive the Au growth into triangles and prisms. But CdS synthesis was performed using polymer- dendrimer which also serves as self-assembly agent.

Chapter 6 devoted to light-induced synthesis. The chapter also speaks about the light-induced synthesis of Ag, Ag-Au alloy nanoparticles. Light-induced synthesis and characterization of ZnO is described.

Chapter 7 describes the crystallization of nanostructures. An attempt to solve the most important questions by using crystal defect theories and explain the paths and ways of crystal growth. Also, light influence on materials discussed and analyzed.

Chapter 8 gives the suggestions for the future works. Light-induced synthesis with more materials and more complicated light-codes. Use of soundwaves and vibrations could give interesting results in the synthesis of nanoobjects.

Chapter 2 Literature R eview

In this chapter, a detailed review is given on the nanomaterial synthesis methods. The most popular and efficient methods are described in detail. Special attention is given to the methods used in this work (photochemical, light-induced) and materials (silver and zinc oxide) that were synthesized in this work. Advantages and disadvantages of each technique are described. Current trends in nanosynthesis that are up to date are analyzed and discussed.

2.1 Introduction

Nanotechnology has greatly influenced science and the lives of most of us already. It includes almost all known disciplines: textiles [30ï 33], mathematics [34, 35], computer sciences [36], biology [37, 38], medicine [39, 40] etc. Synthesis methods are crucial for this type of science. Since the quality of the nanostructures depends also on the synthesis methods it is important to develop new methods and strategies and to continue upgrading the traditional methods. Depending on the size, shape, materials and quality of the nanostructures their properties can change significantly. In most cases it is desirable to have a monodispersive system with a particular size and/or shape of the material [41]. However, there are very few reports regarding chierarchical structures and the formation and growth mechanisms behind them [42, 43]. A range of synthesis techniques are used in nanochemistry: *vapor-liquid-solid* method (VLS), a *sol-gel* method, *hydrothermal* method, *template-assisted* and *photochemical* methods. In this work, we are going to review mentioned synthesis methods and highlight the advantages and disadvantages of each method.

2.2 Vapour -Liquid -Solid Synthesis

The vapor-liquid-solid (VLS) method has been widely studied and used to obtain one-dimensional structures like nanowires. The mechanism was developed 50 years ago and first used in the silicon industry by Wagner [44]. Then starting from the 1 9 9 0 ô s i t was the beginning of the wide use of this method for nanostructure growth after the Lieber [45ï 47] group at Harvard University demonstrated the efficiency of this method. In the VLS process there are three main stages: (a to b) alloying, (b to c) precipitation, (c to d) axial growth (Fig. 2.1). This process runs only at high temperatures and involves vapor-liquid-solid phases of the material and thus is called the VLS process. With VLS it is possible to grow the structures from nanometer to

even centimeter scale. This mechanism requires one very important component: metal catalyst. The problem with this method is that not all the metals can work well. The main requirements for the catalyst materials are: (1) it must form a liquid solution with a component, (2) the catalyst must be more soluble in the liquid phase than in a solid phase, (3) the vapor pressure of the catalyst material over the liquid alloy must be small, (4) the catalyst material must be inert to chemical reactions, (5) the catalyst material must not make an intermediate solid. So the material catalyst must not evaporate during the process, must not react with the materials, must not spoil the reaction and basically guide the materials in the process in order to get the final formation of nanowires. This is the reason why gold works very well for growing Ge, Si, ZnO, nanostructures. The VLS method is popular for the growth of vertical nanowires with less than 100 nm diameter and a length ranging from a few hundred nanometers to a few centimeters. Nanowires found their application in optoelectronics [47, 48] and became very popular since the VLS method can provide both high quality and control over the growth process. Using the VLS process it was even possible to make branched structures [49, 50] which was usually difficult to achieve. It was found that not only gold can be used as a catalyst material thus expanding the borders of the synthesis tactics [51]. In the growth of Si nanowires via the VLS method and using Au as a catalyst leaves deep defects in nanowires.

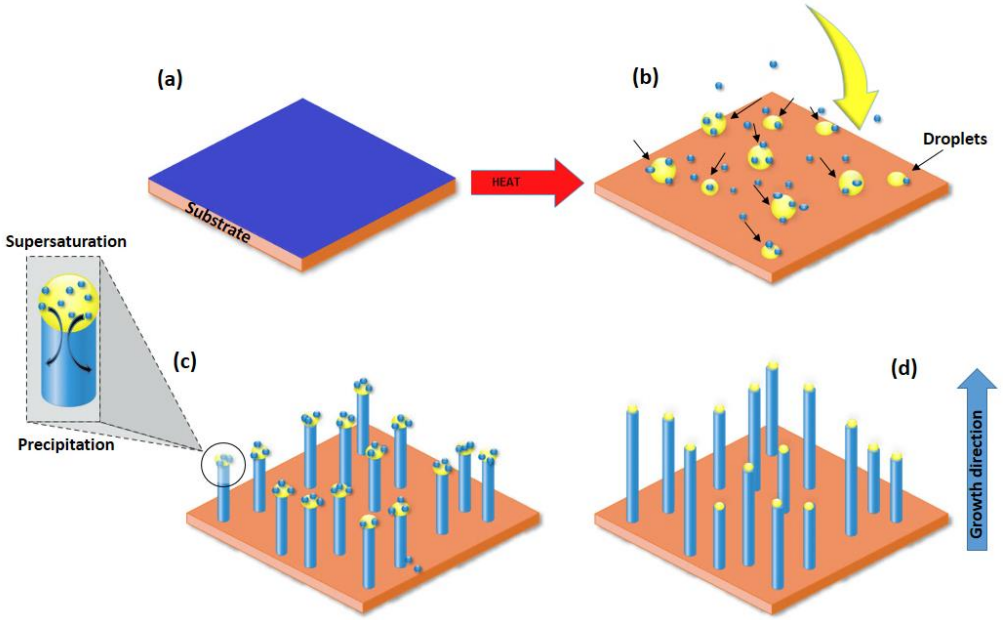

Figure.2.1 VLS method process in growing 1D nanowires. Step (a): substrate with the material on it. Step (b) heating up the substrate and dissolving-evaporating the material. Step (c): precipitation. Step (d): growth of 1D nanostructures (whiskers in the case depicted).

Also cleaning the final product and the equipment from gold is quite difficult [51]. Si wire synthesis was accomplished with other materials such as Ag [52], Al [53], Co [54], Cu [55], Fe [56], Ga [57]. The growth rate determining factor is the speed of incorporation of atoms into the nanowire and can be controlled via processing conditions. In this process (at high temperatures) van der Waals force and Ostwald ripening force are the driving particles to larger clusters and the formation of large droplets. Since every particle is trying to attain lowest possible energy and agglomerate, it requires precision in preparation, positioning them and heating the surface during nanowire growth. As it was mentioned before sometimes catalyst materials are not very efficient because they cause impurities (Au for instance) and thus permanent damage to the final product-nanowires. By increasing the amount of impurities of the catalyst material in the band gap causes degradation of optical properties of the nanowires which is so important for the industry. It was found that Au can be replaced by Pt [58ï 61] and causes even higher growth speed under the same conditions. Ke et al. synthesized Si nanowires using Al as a catalyst [62].

2.2.1 Issues with VLS Method

The same group faced specific problems related to the VLS synthesis method [62]. The basic issue was with Al oxidation and more airtight system design was required. Scientists used temperatures ranging from 500 ^{0} to 600 ^{0}C and H_2 and SIH_4 and it was found that these materials were reducing the oxidation but not completely eliminating it. Growing interest to the catalyst-free VLS method increased a number of works in this area. This useful method solves catalyst contamination problem and can be applied to a number of materials [63, 64]. Interestingly the self-catalytic process was reported in 2014 by Yu et al. [65]. The metal oxide nanostructures growth process was based on electron beam evaporation. The condensed electron beam was a decomposing metal oxide source and was performed with In(Sn), Ga, Al grown on Si. The control of the structures can be achieved by the variation of the synthesis time and becomes optimal after 150 seconds [65].

2.2.2 Advantage of VLS Method

A key role of the VLS synthesis in nanotechnology is the ability to grow vertical wires that have optoelectronic properties desired for photovoltaics, LEDs and electronics. Hochbaum et al. synthesized Si vertical nanowire arrays [66]. The nanowires were around 40 nm in diameter and Au colloid nanoparticles were used as a catalyst

material. The nanowires were uniform and to demonstrate the flexibility of the method researchers grew them directly into microchannels. However, deposition of nanoparticles onto any surface is always random and precise control of the nanoparticle deposition still remains a challenge. Other similar experiments were performed by different groups but they included work with dangerous chemicals such as hydrofluoric acid (HF) for cleaning purposes [66, 67]. Orlandi et al. [68] reports growth of SnO_2 nanobelts and dendrites by VLS method. The synthesis was performed at 1210^0 C in the carbothermal process in a sealed tube furnace at N_2 gas flow. Basically, researchers mixed SnO_2 and carbon powder and heated it up in the furnace for 2h. The resulting product was nanowires with branching out elements resembling branch-like structures. This experiment required small amounts of chemicals and high temperatures only. The major issue is the control of the size and width and achieving the diameter of less than 10 nm of the nanowire was a great challenge. The classic problems with this method are still the setup of the experimental equipment which is usually expensive and requires specific conditions such as fume hoods and inert gasses. Also as was mentioned before air-tight setup could be an issue which can lead to the imperfections of the nanowires and degradation of their optoelectronic properties. Use of high temperatures requires monitoring and control and also time and the properties of used materials are of great importance.

2.3 Sol-Gel Synthesis Method

The sol-gel process is the name for a group of synthesis used to synthesize usually metal oxide nano/micro structures. Normally in this process, sol and then the gel is formed in order to get the final product. The sol-gel process can be aqueous involving water as a main solvent or non-aqueous which involves organic solvents [69].

2.3.1 Aqueous Sol-Gel Process

This synthesis method is one of the most complicated due to the high number of chemical processes involved [70]. To control this process many parameters are involved: pH [71], temperature [72], hydrolysis and condensation rate [73], time [73], the concentration of anions, the rate of oxidation, metal oxide precursors [73] and even the method of mixing. In the aqueous sol-gel process to obtain sol ï highly dispersive colloidal system condensational or dispersive methods are used. During this process, an ñelastic solidò is formed. The then network synthesis of metal oxides, it is like a polymer connection from metal to -oxo (M-O-H)

or -hydroxo (M-O-M) (M-metal) bridges [69]. Using this method, it is possible to synthesize various types of metal oxide nanostructures including: Si, Ti, Zn, Cr, Vn, Al, Sn, Ge etc. The initial solution usually contains either metal alkoxides (non-aqueous) or chlorides (aqueous) as precursors (Fig.2.2) then depending on the desired result the solution is either coated on a surface or it undergoes hydrolysis and polymerization states. The next step is wet gel and the removal of the solvent by evaporation either at room temperature or slightly heating up the material. The solvent can be water or any organic solvent but in most cases it is ethanol. The extraction of the material by centrifugation is also efficient or natural precipitation is used. In general, we can summarize these steps: 1) preparation of a solution, 2) conversion of prepared solution to sol, 3) aging, 4) shaping, 5) thermal treatment. At the final stage, we have an inorganic interconnected network- gel (sol-gel transition). The reason this method is one of the most popular in synthesis is the ability to shape the material into almost any desired form: fibers, films, powders, monoliths and convert it into the ceramic material by heat treatment.

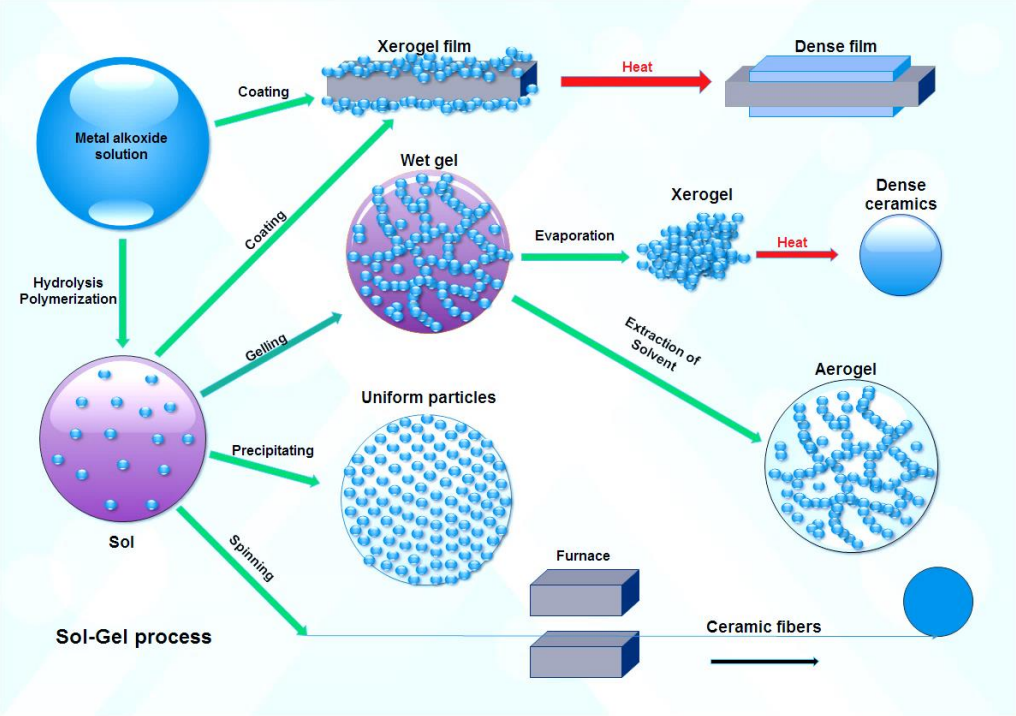

Figure. 2.2 depicts the process of sol-gel synthesis. First steps show the initial solution (metal alkoxide in our case). Other steps involve coating and obtaining xerogel film or directly using the hydrolysis process and polymerization leading to the formation of sol. After sol is obtained coating can be performed (depending on the result required). The last step processes involve evaporation and creation of xerogels or aerogels depending on evaporation techniques. The final product can be dense film, ceramic or fiber.

2.3.2 Issues with the Aqueous Sol-Gel Process

The major problem is the control of the reaction rate. The reactions in this process are simply too fast for most of the transition metal oxide precursors. Hence it results in the uncontrolled formation of shapes and sizes of metal oxide structures. It is also important to mention that every metal oxide precursor has its own reactivity thus making every synthesis process specific for every material. To overcome these problems and drive the reaction process in a more controlled way additives such as carboxylic acids are used. The role of these acids is to decrease or modify the reactivity of the metal oxide precursors and act as chelating agents. This method used in synthesis and coating of ceramics has proven to be very efficient because it gives the ability to coat almost any surface. However, post-treatment prevents precise control of the crystal size and shape. The fundamental issue with this process is the sensitivity to many factors which basically makes the process impossible to control and such parameters as the size distribution of shape of the material is barely controllable. Non-aqueous sol-gel synthesis can overcome some problems persistent in aqueous synthesis method by replacing water with organic solvents. Non-aqueous sol-gel synthesis. In this process, the transformation occurs also in liquid media but organic solvents are replacing water. The precursor. Typically, it is a metal alkoxide or acetate. To define a typical formula of used precursor chemicals: R-O-M, H_3C-O-M, where R is the organic substituent. In the aqueous process normally metal gets oxygen from the water and in the non-aqueous process the oxygen comes either from solvent or is provided by the organic constituent of the precursor. In other words, the second possibility occurs when the metal oxide precursor molecule is a new molecule. part of its

2.4 Hydrothermal Synthesis Method and ZnO

Hydrothermal synthesis is a widely used method usually to obtain nano/micro structured ZnO [74-76]. In most synthesis procedures the metal precursor is added into distilled water. The second process is usually the addition of either donor of oxygen (in the case of oxides synthesis) or the reducing agent (in Au or Ag synthesis). The last step is heating and stirring the solution for a couple of hours. The heating up is required to complete the synthesis process and sometimes even to speed up the growth of nanoparticles. Heating up spend also can affect the shape and size of the materials. Fig.2.3 depicts the chemical glass and the steel autoclave used in hydrothermal synthesis. A common issue with the autoclave is that the solution inside is heated up

in a furnace and without stirring. The temperature applied to autoclaves usually ranges from 80^0 to up to 250^0 C. Chemical glass or vial that can stand a few hundred degrees are also widely used in hydrothermal synthesis. They can be used to precisely control the concentration and even modify the growth during the process by simply adding the salt into the solution. Stirring can be precisely controlled as well and is usually a few hours in the synthesis process. Using this method nanostructures of ZnO [77], SnO_2 [78], TiO_2 [79], including sulfides [80] (ZnS, CdS, PbS, CuS, FeS, BiS) etc. were successfully synthesized with various shapes. This method provides good quality and size distributions of synthesized products also allowing to

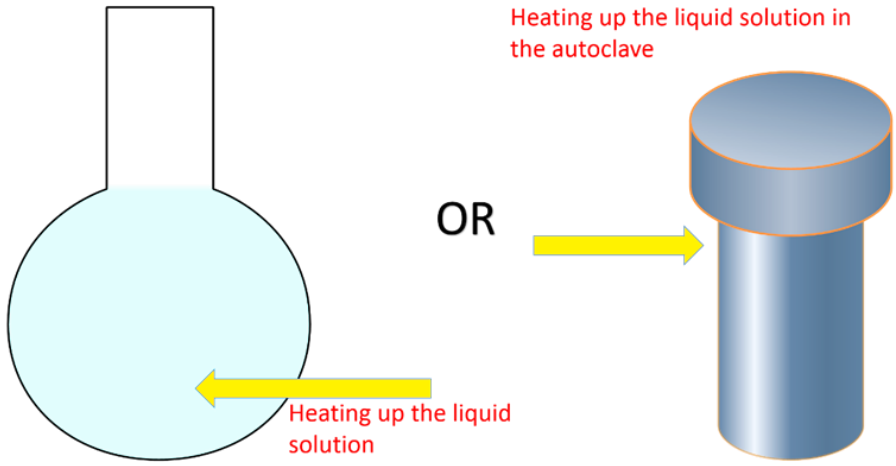

Figure.2.3 traditionally chemical glass and steel autoclave used in hydrothermal synthesis processes.

control the synthesis process by varying the synthesis time, pH, concentration and impurities of the solution. The first report on the hydrothermal method dates back to 1845 when German geologist Karl Emil von Sch a f h [81] reported microscopic quartz crystals grown in a pressure cooker. The term Hydrothermal comes from ancient Greek (hydro- i ŭ x water) and (thermos- d Ů J ewarm/hot) and is purely of geologic origin.The hydrothermal method can be used to synthesize many types of nanoparticles but became very popular for the synthesis of metal oxides [81ï 85]. SnO_2 was synthesized using this method in a variety of works [86ï 88] and proven to obtain high control over the sizes and shapes of the structures [76, 89]. Wang et al. synthesized tin oxide nanoflowers on the surface of indium tin oxide in the presence of PVP [90]. Structures were grown in autoclave at 200^0 C for 12h. The obtained product was around 300nm in width and resembles hedgehog-like structures. Along with PVP solution contained NaCl. The structure pathway is associated with the

synthesis time and the PVP polymer persistence. Patil et al. reported a hydrothermal route in the presence of hydrazine at 100^0 C for 12h [87]. The resulting product was spherical nanoparticles of 40 to 70nm width looking like clumps of rice and spherical particles together. The proposed reaction was basically the reduction of Sn precursor by hydrazine (few chemical reaction steps process). Lupan et al. report SnO_2 nanofibers with lengths of 10-1 0 0 Õ m a n d-100wmid[86]h In this synthesis, NH_4OH was used and the study suggests the chemical played a major role in the synthesis.

2.4.1 Synthesis Scheme and the Morphology

Scientists suggest the formation of amphoteric hydroxide $Sn(OH)_4$ and dissolution in NH_4OH followed by the formation of $Sn(OH)_6^{2-}$ ions and the formation of SnO_2 after the hydrothermal process. The study suggests that Sn ions play a key role in the formation of the thickness of nanowire and are found to be optimal at 1:20-25. All the mentioned experiments synthesizing SnO_2 suggest that the control over the morphology of the nanostructures can be achieved by changing either the chemicals or the processing conditions like temperature. Du et al. reported the formation of SnO_2 hollow microspheres in the autoclave at 160^0 C for 16 hours [91]. In this synthesis, researchers used methenamine($(CH_2)_6N_4$) and carbamide ($CO(NH_2)_2$) along with $SnCl_4$. They also controlled the pH by the addition of sodium hydroxide (NaOH) and having pH in the range of 9-1 1 . T h e m i c r o s p h e r e s w e r e o f a consisted of small nanospheres of 70 to 150nm in diameter.

2.4.2 Reaction Scheme and Morphology

The proposed reaction suggests that $CO(NH_2)_2$ was hydrolyzed into CO_2 and NH_3L H and only then the formation of nanosphere occurred. The process of the final microsphere formation remained unclear since it is structural and already consists of formed nanoproducts. However, researchers speculate that formation of the microsphere could be attributed to the microbubbles of CO_2 during the reaction. Basically, a microbubble was solving the agglomeration issue at that scale. The nanospheres were agglomerating around the microbubble thus creating the shell of SnO_2. This work shed some light on the synthesis of SnO_2 via the hydrothermal process. Changing the size and shape of the nano or microparticles and achieving high control over the synthesis process was always the main purpose of the nanochemistry as such. Chen et al. reported the hydrothermal synthesis of SnO_2 with different

morphologies [92]. Researchers obtained pine needle-like, nanospheres, nanosheets and grape-like nanostructures. Every structure had different preparation steps also varying in chemicals and processing parameters such as time and temperature. For the preparation of pine needle-like structure, $Na_2SnO_3 \cdot 3H_2O$ and NaOH were used. The later synthesis was followed by the addition of $(CH_2)_6N_4$ and in all four cases synthesis was performed in a Teflon-lined stainless steel autoclave. The synthesis temperature was 180^0 C for 24h. Fabrication of grape-like structures included the same procedure steps and the difference was the amount of chemicals and the tin precursor which was $SnCl_4 \cdot 5H_2O$. Other two cases of spherical and sheet-like structures had the same processing conditions: 180^0 C for 12h. Also, the same precursors were used $SnCl_2 \cdot 2H_2O$ along with NaOH and $Na_3C_6H_5O_7 \cdot 2H_2O$. The main difference was the amount of chemicals and in the sheet-like preparation procedure magnetic stirring was used.

2.4.3 Morphology Influencing Factors

It is not possible to answer the question whether the stirring could cause such changes in morphology since the solution with chemicals always has Brownian motion between the particles and molecules. In the hydrothermal synthesis of oxides usually, the acidity (pH) is one of the main factors determining the synthesis results [93]. But the authors did not focus on explaining the SnO_2 morphologies but rather on gas sensing properties such as H_2. As mentioned before the hydrothermal synthesis method is widely used to synthesize metal oxides with various shapes but probably the most popular material is zinc oxide (ZnO). This material has grown in popularity both for nano and microstructures and a hydrothermal method is a powerful tool in the synthesis of ZnO. In a typical hydrothermal synthesis of ZnO traditionally the zinc precursor and NaOH are involved. For the zinc precursor usually, it is zinc acetate or zinc nitrate and the NaOH serves as an oxygen donator.As mentioned previously pH and other factors like synthesis time and temperature play a key role. The properties of ZnO depend on the shape, size and surface structure of the material. Control of the synthesis process and also synthesis modelling are essential. Amin et al. reported work that focuses on the influence of pH, temperature, concentration and time in ZnO synthesis [94]. They synthesized different types of nanostructures like flowers, urchin-like, rods and tetrapod structures. The report mainly focussed on pH of the solutions. The chemicals used were zinc nitrate and $(CH_2)_6N_4$ for the pH control HNO_3 and $NH_3 \cdot H_2O$ or HCl

and NaOH were used. For the pH control depending on the materials approaches referred as procedure A and B. The pH values were set for 1.8, 2.5, 3.5, 4.6, 6.6, 8, 9.2, 10.7, 11.2 and 12.5 i.e. from strong acidic to strong basic solutions. It was found that the main controlling parameters were the pH and the temperature. By changing the temperature it is possible to change the morphology of the nanostructures. They obtained nanosized structures: tetrapods, flowers-like and urchin-like structures at high pH values pH=8 or more. While lowering the acidity led to the formation of the rods and even film-like structures. Also they found that by increasing the temperature the aspect ratio of nanorods increased [94].

2.4.4 The Time as Synthesis Influencing F actor

The time factor was also very important and by increasing the synthesis time the length of the nanostructures also increased. At the synthesis time of 1h the length of the nanorods were around 500nm and by increasing the time to 3h the length increased to 1 Õm. Further increasing the growth time
It seems to be logical that at the constant concentrations and temperature the structures continue to grow. However, if we imagine the solution with ions and molecules of the chemicals inside it is also logical that the concentration should always decrease while the growth continues.

2.4.5 The Influe nce of Precursor

The influence of the precursor concentration is pointed out very clearly stating that the increase of the concentration of the precursor (zinc nitrate in this case) leads to the formation of polycrystalline films. While lower concentrations lead to the formation of nanowires. Researchers found that the length becomes constant at the concentration of 200 mM which basically suggests that there is a limit for ZnO growth [94]. Increasing the concentration led to the formation of film. This observation allowed to conclude that a linear relation can be drawn between the concentration and nanorod dimensions. This work actually showed the connection between the parameters such as time and concentration. However, the precursor and pH controlling chemicals seem to be the main parameter since the aspect ratio and the shape can be controlled by just adjusting the concentration. While the time and the temperature seems to be efficient only in affecting the aspect ratio of the structures. Other interesting works in ZnO hydrothermal synthesis were performed by various scientists using chemicals such as already mentioned before $(CH_2)_6N_4$ and other types including polymers and organic

molecules. Sugunan et al. investigated the influence of hexamine on the growth of the ZnO structures [95]. They used temperature 60-95^0 C for 24h to synthesize the few micrometer nanowires with around 30 nm thickness. The proposed model for this growth was the attachment of hexamine molecules attached to non-polar facets of the crystal thus leaving polar facets to grow and form the nanowires with high aspect ratios. It seems that for synthesis of particular shape of ZnO the extra-templating chemical was required.

2.4.6 pH as Morphology Influencing F actor

Some works report hydrothermal synthesis of ZnO without any template. Bhat et al. reports synthesis using zinc precursor, methanol and NaOH [96]. They maintained the solution in an oven for 8h at 160^0 C. The difference of every sample was the pH and they obtained spherical particles with a 100 nm diameter at pH=8, elongated cracker-like structures at pH=12 with a diameter of around 100 nm and 500 nm length. Varying the amount of chemicals but keeping pH=8 they also synthesized rods and spherical particles together ranging from 100 nm to 450 nm. At pH =9 the dominant structures became spherical nanoparticles with very few nanosized rods. While it is still possible to synthesize ZnO nanostructures without the aid of any other molecule obtained structures in such way usually have defects or size and shape distributions and might exhibit different properties. Hence this is not always desired and more precise approaches are required such as the use of hexamine.

2.4.7 Influence of Additives on ZnO S ynthesi s

Over the past fifteen years hydrothermal synthesis of ZnO using additives gained great popularity because of its effectiveness and the possibility to modify by simply changing the amount of additives. Chen et al. synthesized ZnO with various shapes and using different additives [97]. The temperature was chosen to be from 100^0 to 220^0 C and the time from 5h to 10h. The additive was chosen 1,6-Hexadianol and it resulted in the formation of rod-like structures with various sizes and lengths basically ranging from 300 nm to 700 nm. The thickness of the rods also differs from 30 nm to 70 nm. When additive was previously mentioned hexamine ($(CH_2)_6N_4$) the result was snowflake-like and the size was around 200-300 nm. Using ethanolamine as an additive polyhedrons were synthesized with sizes from around 150 nm to 220 nm. Also they observed the change in shape from rod to polyhedral after increasing the temperature. The researchers observed and described the synthesis however they did

not explain the shape formation behind the process. Zhang and Mu have grown ZnO homocentric bundles using zinc acetate and NaOH with the addition of polyether [98]. The synthesis was performed at 160^0 C for 16h in an autoclave. The shape of the ZnO crystals were attributed to the growth habits of ZnO and the influence of polyether. The role of polyether is proposed to be templating the zinc-containing molecules and due to the process when $Zn(OH)_2^{4-}$ is surrounded with PEO-PPO the resulting growth makes the homocentric bundles. These structures are made of hexagonal and pyramid-like ZnO crystals that grow due to ZnO growth habit.

2.4.8 Different M orphologies of ZnO

Lu and Yeh synthesized ZnO powder with temperature at 200^0 C and used ammonia which also served as a pH controlling chemical [99]. The heating time was ranging from 30mins to 2h. The obtained powder after SEM characterization revealed microsized rice-like ZnO structures. Also they observed that increasing the pH from 9 to 12 the aspect ratio of the structures increased f o r m i n g Another simple method was proposed which led to the formation of ZnO various nanoparticles by Music et al. [100]. The nanoparticles were mostly spherical and the synthesis procedure included the use of tetramethylammonium hydroxide (TMAH) which led to 10-20nm nanoparticles along with dendron looking like structures of 200 nm and larger in size. Synthesis methods that are most simple and do not require high temperatures or complicated polymer mixtures make the hydrothermal method one of the most attractive both for science and industry. Cunha et al. demonstrated synthesis of urchin-like structures which are referred as nanoflowers in the article [101]. They used zinc chloride and ammonium hydroxide and the synthesis was performed at 90^0 C pH=10.5 for different amounts of time. All the structures were urchin-like with slight differences: thickness, density of the nanorods that come out of the center, sharpness of the nanorods and packing of the structures which also could be accidental. The experiments were performed for different amounts of time ranging from 15 minutes to up to 72 hours. The results revealed that at a synthesis time of 72h the nanorods were the sharpest in comparison to other samples and the 30mins, 2h and 6h synthesis showed nanorods of urchin-like structures having the smallest aspect ratio. Synthesis in supercritical water was performed by Viswanathan and Gupta [102]. Basically they oxidized zinc acetate in supercritical water in less than a minute. The obtained nanoparticles were with sizes ranging from 120 nm-320 nm in diameter. Li et al.

synthesized different shapes of ZnO ranging from nano to micro size [103]. Two different precursors were used: ammonia referred to as A and ammonia and zinc nitrate referred to as B. The synthesis temperature was 80^0 C for 12 or 24 hours. In the case of A precursor nanowires were obtained with different diameters and lengths and using the B approach thicker nanowires and hexagonal shaped nanowires were obtained. It is important to mention that all the nanowires were synthesized on a large scale on zinc foil and all of them were vertically aligned. They report that sharp wires were obtained at alkaline solutions while more flat within less alkaline medium.

2.4.9 Synthesis of Complicated ZnO Structures

Synthesis of more difficult structures has always been a challenge because of the different properties that those structures exhibit. One of the most attractive ZnO nanostructures is a flower-like structure which has a center and branching out leaves or Dendron-like shapes. One of the very unusual works was performed by Shao et al [104]. Flower-like structures were synthesized using zinc chloride and ammonia. Copper plate was immersed into the reaction solution before the heating up. The synthesis temperature was 95^0 C for 2h. The obtained structures had plates branching out from the center and resembled roses 30 microns in diameter and 150 to 250 nm thickness of the leave (fragment of that rose). Important to notice that rose-like structures were in ordered manner and distributed over the sample very uniformly as indicated by SEM. While the addition of polymers could be explained by the template-like role the use of ammonia raised the question of the chemical reaction within the solution. According to ref [84] this reaction could be written as:

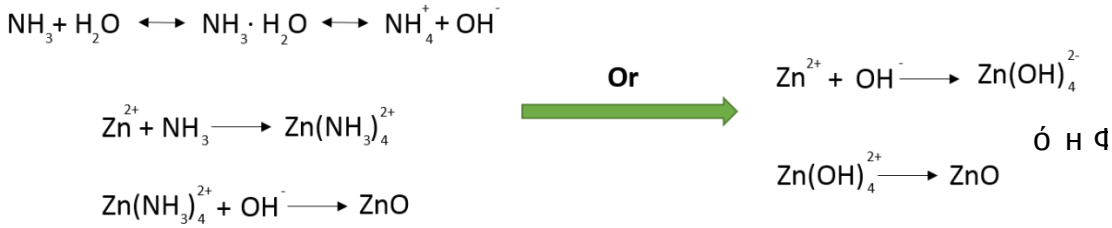

As we can see ammonia is creating intermediate products which later form ZnO structures. In the case when hexamine is used it is known that during thermal decomposition of HMT it releases the hydroxyl ions that are very important in the

formation of ZnO. So the reaction with hexamine can be written in the following way [84]:

$$(CH_2)_6N_4 + 6H_2O \longleftrightarrow 6HCHO + 4NH_3$$

$$NH_3 + H_2O \longleftrightarrow NH_4^+ + OH^-$$ ó HỨ

$$2OH^- + Zn^{2+} \longrightarrow ZnO + H_2O$$

Synthesis of microsized urchin-like structures (nano-flowers referred in the article) were synthesized using zinc acetate and NaOH at 90^0 C for 30 minutes by Wahab et al [105]. The structures were basically sharp around 300nm in diameter. Structures were uniformly dispersed over the sample and the size and shape distribution was very uniform. Another interesting work that showed flower-like, urchin-like and various other shapes ZnO structures was performed by Zhang et al [106]. Researchers found that such factors as the polarity and the saturated vapor pressure of the solvent are the key factors in shape and size formation of the final product. Also influence of already mentioned factors such as pH, temperature and time were confirmed in this work. Still the growth reasons and the directions are not clear. And the growth habits of the crystals should be well investigated.

2.4.10 Growth Mechanisms of ZnO

One of such works towards investigation of the growth habits of the crystals was made by Li et al [103]. Researchers used zinc acetate and ammonia hydroxide. The autoclave was a stainless steel silver lined tube type with a valve for gas relief at the upper part. The temperatures applied ranged from 200^0 to 350^0 C. The obtained structures were hexagonal prism-like wires with micron sizes. The growth habit of the ZnO structures are related to the growth of crystal faces and they are related to the elements of the coordination polyhedron at the interface. The article suggests that ZnO can grow either faster or slower in some directions. Depending on the solution concentration and pH ZnO crystals can take different shapes. For instance, the fastest growth direction for ZnO is [0001] thus providing nanowire growth in most of the synthesis. The growth processes and the growth habits will be discussed in detail in the Results and Discussion chapter. The hydrothermal method is not limited and can be used not only for oxides.

2.5 Hydrothermal Growth of Ag Structures

Another material that is widely synthesized using the hydrothermal method is silver. Zou et al. synthesized different shapes of silver nanoparticles using the hydrothermal method [107]. The synthesis was performed in the autoclave using $AgNO_3$ and ammonia. Scientists synthesized various shapes of silver nanoparticles: spherical, triangles, rods, hexagons. It is important to mention that along with the chemicals PVP was used as well. Authors believe that it was PVP that caused both the templating and the reduction. Also they found that the variation in concentration for both PVP and $AgNO_3$ can change the shape and size of the nanoparticles. Another hydrothermal work on silver nanoparticles was performed by Aksomaityte et al [108]. For this synthesis a counter-current pipe reactor was used. Silver acetate and PVP were used with different concentrations and at different reactor temperatures. The synthesized particles were 30-40 nm in size as reported. Most of them were spherical in shape. Yang and Pan used the hydrothermal method to synthesize silver and chosen sodium alginate both as a template and the reducing agent [109]. They used different temperatures for 6h and 12h of synthesis. The obtained particles were spherical when the synthesis temperature was 100^0 C for 12h and in the case of 120^0 and 180^0 C mixture of triangles and hexagonal nanoparticles with various size distributions. Kometani and Teranishi demonstrated Ag nanoparticle synthesis in a flow-type reactor system [110]. The reactor allowed the rapid mixing of two solutions: one containing silver precursor and another one a reducing agent. The second solution contained PVP and the nanoparticles were triangles, rods and sphericals with sizes of around 200 nm and 500 nm for the rods.

2.5.1 Hydrothermal G rowth of Au and CdS Nanostructures

Along with silver, synthesis of gold also has been reported. Liu et al. used the hydrothermal method to synthesize gold nanoparticles with narrow size distributions [111]. For this synthesis chloroauric acid $HAuCl_4$ and l-histidine $C_6H_9N_3O_2$ were used. The temperature used was from 65 ^{0}C to 150 ^{0}C and the size distribution of the particles were 11.5 nm which is not easy to synthesize using other methods. Some particles were triangle-like with rounded corners (around d=10 nm). Another hydrothermal method for Au synthesis was performed by Liu et al [112]. The pH was controlled and the dendrimer of PAMAM type was chosen as the stabilizing agent. The particle sizes were around 5.6 nm which was a high achievement considering the agglomeration and other factors at that scale. Cadmium sulfide nanostructures and nanoparticle can also

be synthesized via the hydrothermal approach. Xiang et al. synthesized CdS flower-like, leave-like and branched structures [113]. The reaction time, temperature found to be most influential and found to be optimal was 180 ^{0}C at a particular concentration. The study showed that increasing the synthesis time the structures were more and more complicated. The role of pH on CdS hydrothermal synthesis has also been reported [114].

2.5.2 Microwave -Assisted Synthesis

One of the processes that can be associated with the hydrothermal process is Microwave-assisted synthesis. Instead of producing heat by conventionally heating up the solution it is heated up by microwaves in an oven. Using this method, it is possible to synthesize the variety of materials. Some of them we are going to review briefly. One of the main advantages of this approach is that the solution is heated up immediately since the microwaves transport the energy through the materials. CdS microwave assisted synthesis was performed by Caponetti et al [115]. The synthesis was performed in an oil-water microemulsion at 2.45GHz frequency and 22-30W power of the oven. The results obtained were rather outstanding since they obtained very small 2.7nm CdS crystals. They maintained 35 ^{0}C temperature during the synthesis process and concluded that due to the interaction between the electromagnetic field and the dipoles of the water eventually initial faster growth occurred. Synthesizing CdS with such small sizes was always challenging and usually required either a very well controlled synthesis processes or a very good templating since nanoobjects at that size tend to aggregate or due to Van der Waals forces agglomerate rapidly [116, 117]. Esmaili and Habibi-Yangjeh synthesized CdS in 4-6minutes [118]. They used 1-ethyl-3-methylimidazolium ethyl sulfate (RTIL) and water mixture. ESEM micrographs reveal that the sizes were ranging from 50nm to up to few hundreds of nm. Various nano and micro ZnO structures were synthesized using zinc nitrate and pyridine via microwave hydrothermal synthesis [119]. The synthesis time was 10mins and the temperature 900 C. Changing the concentration of pyridine it was found that shape and size can also be controlled. Motshekga et al. demonstrated microwave synthesis of metal oxides supported on carbon nanotubes [120]. Zhu et al. demonstrated the synthesis of tellurium nanorods and nanowires [121]. As we can see the hydrothermal microwave-assisted syntheses basically do not have limits in terms of the materials that can be used and the high quality of the product that can be

achieved. To understand the internal processes we must first ask: what are microwaves? Microwaves are electromagnetic waves with frequencies of 300MHz to 300GHz. When a portion of the microwaves hits a polar molecule, such as water for instance, the water molecule is trying to orientate with the electric field of the wave Fig. 2.4. After the orientation process has occurred and the dipolar (H_2O) molecules orientate they have already lost the energy portion due to the molecular friction and this energy is then transferred in the form of heat [122, 123].

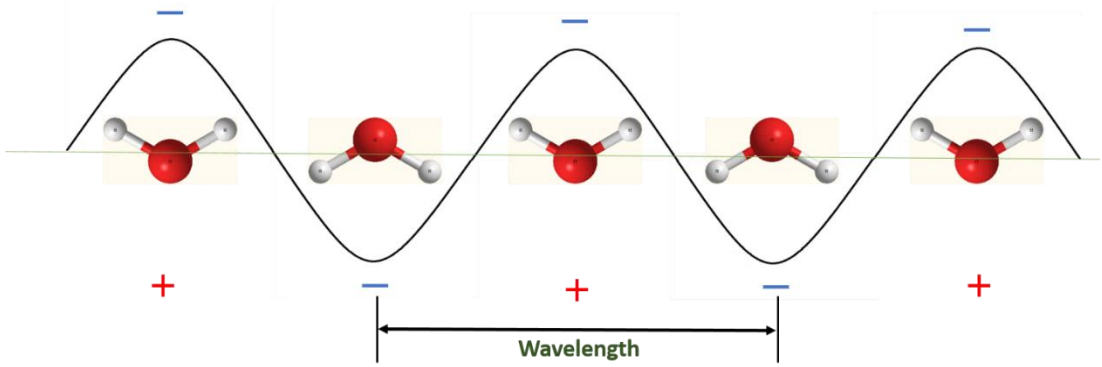

Figure. 2.4 orientation of water molecules in an electric field after the microwave hits the water.

Water is a good microwave absorber with a relaxation time of 9 Ĭ 112 s at 200 C and a relaxation frequency of around 18GHz [123]. Microwave-assisted hydrothermal synthesis provides uniform and rapid heating of the solution causing the synthesis of a uniform nanosized object with small size distributions.

2.6 Photochemical Synthesis of N anoparticles

Another important method that is used in nanosynthesis is the photochemical method. It is believed that light can cause reduction reactions with the nanoparticle precursors. Also, it is important to mention the fact that photochemistry cannot be used on all materials. Traditional photochemical synthesis is the synthesizing of silver nanostructures. Basically, this method is a liquid chemistry method and involves traditional (nitrates, chlorides etc.) chemicals dissolved in a liquid medium with or without the addition of the reducing agent. The silver nanoparticles were triangular shaped after exposing the solution containing silver nitrate and sodium citrate to the green light. The synthesis was done with Light emitting Diodes (LEDs) and with a laser as a source of light.

2.6.1 Wavelength of Light Influence on the Synthesis

J., Zhang et al. found that depending on the wavelength of light it is possible to control the aspect ratio of the nanorods [124]. Their photosynthesis is based on a seed-mediated approach. To synthesize seeds $AgNO_3$ and BSPP solution was used and irradiation with UV light of 254 nm. Then the solution was added to the mixture of $AgNO_3$ and sodium citrate. The irradiation was performed for 24 hours using a 150W light source and filters with filtering from 600 nm to 750 nm +-20 nm. The result yielded in very uniform nanorods with pentagonal cross-sections. The work showed that increasing the excitation wavelength from 600 to 750 nm the aspect ratio of nanorods tends to increase. Maretti et al., made another photochemical synthesis method that was performed in THF and in toluene, results showed high fluorescence of Ag nanoparticles [125]. The synthesis was done in the nitrogen atmosphere and in the air. The precursors were silver acetate with cyclohexylamine and a UVA was used as the light source. According to the report, the solution showed the formation of nanostructures in around 3 minutes (by changing the color of the solution). TEM images indicated only spherical shape of the nanostructures and the difference in size with each solvent. Nanoparticles synthesized using THF were twice smaller as that with toluene. In the case of the reaction with THF particles size 5 +-2nm and with toluene around 10+-2nm. The presence of cyclohexamine proved to have an influence in synthesis as another solution containing toluene and hexadecylamine was proven to increase the size distribution. This approach could be useful if fluorescent NPs were needed. Pa
UV lamp was used as well [27]. The main difference with previous methods is that citrate-capped seeds were used. Authors hypothesized that the synthesis occurred due to photoelectron transfer from citrate to Pt nanoparticle seed. The resulting Ag morphologies were nanorods and nanoparticles. Exposure to UV light with variation in time for every sample showed a significant difference in the resulting product. Exposing for 45 minutes to UV formed nanoparticles and clump-like structures and increasing the exposure time to 60 minutes gained nanorods with great aspect ratio. Nanorods were of around 100 nm thick and 5-6 micrometer in length. Further based on the work done by Redmond et al [126] the reaction was explained in the following way:

$$\text{Citrate} \xrightarrow{hv} \text{acetone-1,3-dicarboxylate} + CO_2 + 2e^- \qquad \text{ó нứ}$$

This process according to the authors leads to the formation of Ag nanostructures with extra electrons and the reducing source for Ag^+. This experiment suggests an interesting reaction pathway since the citrate is proposed to be other photochemical processes basically should be coming out from this perspective as well.

2.6.2 Shape of the Nanoparticles

However, there is no explanation on the dependence of excitation on the shape of the nanostructure. Pietrobon and Kitaev synthesized decahedral silver NPôby using $AgNO_3$, sodium citrate, PVP, L-arginine and $NaBH_4$ [127]. The nanoparticles were first grown using a chemical reduction of $NaBH_4$ and afterward the solution was exposed to a metal halide lamp (white) of 400-watt power. An experiment was also done with a blue filter which led to the formation of smaller decahedra NPôTshe reaction was monitored using an UV-vis spectroscopy. The results showed that increasing the time of exposure to the light from 2 to 15 hours the size of decahedral NPôs was ranging from 35 nm to 45nm res described to be essential. PVP makes stable nanoparticles and the arginine accelerates the photochemical transformation process. While $NaBH_4$ is a well known strong reducing agent widely used in nanochemistry. In thermal synthesis decahedra nanoparticles do not form so the conclusion is that the light is essential for this synthesis. Another very similar photosynthesis was performed by Zhang et al [128]. they used 150 W halogen lamp the filters were 500 +- 20nm, 550+-20 nm and 600+-20nm and 650+-20nm. The solution also contained $AgNO_3$, sodium citrate but the difference was in the use of BSPP and NaOH. The results were nanoparticles with different shapes: triangular bipyramids, triangles and spherical NPôTstriangles and spherical NPôs were observed after stopp respectively. These results basically suggest that the light is playing only the role of force to make a chemical reduction. R., Jin et al. Reports synthesis of nanoprisms also using silver nitrate, sodium borohydride and trisodium citrate then the addition of BSPP helps to form the nanoprisms [129].

2.6.3 Influence of T ime and Light on the Nanoparticle Growth

Light and time also has an influence over all growth process. For the irradiation a 40W fluorescent lamp was used in [129]. They found that increasing the irradiation time from 55 to 70hours the triangles grow more uniform and basically no spherical particles were observed. Most of the photochemical synthesis of silver nanoprisms, nanoparticles, nanorods includes the use of $AgNO_3$ and $NaBH_4$ for the formation of seeds at the initial stage. Since atoms and small clusters attach to the bigger objects inside the colloid the seeds are required. During the growth process the role of light was being introduced. The light can transform spherical nanoparticles into triangles and it is also believed that the growth is mainly influenced by light.

Possible interpretation. Later R., Jin again reports a very similar synthesis procedure that their group used before (regarding the chemicals) [130]. The main difference is that they used a dual-beam illumination this time to grow the nanoparticles. They state that all the process is driven by surface plasmon excitations and the whole process can be controlled by simply changing the wavelength. The plasmon excitation leads to the fusion of the NPôs or the termination of by light. They used a 150W xenon lamp with a 12W output and optical filters for 50 h. The TEM analysis showed that nanoparticles had two distributions of nanoprisms: the smaller particles with an edge of 70+-12nm (type 1) and the larger ones 150+-16nm (type 2). The thickness was observed to be the same for both types of nanoprisms. The process explained with dipole resonance of Ag nanoparticles. The control of the secondary wavelength allows the control of the size of the nanoparticles due to bimodal growth. Bastys et al. used light emitting diodes to grow silver nanoprisms [131]. The nanoprisms exhibited strong absorption in the IR region. The wavelengths of LEDs were: 518 nm, 641 nm, 653 nm. This work also confirmed the influence of longer wavelengths enabling the formation of the side length of the nanoprism. The size of the structures was about 150 to 200 nm (edge length). To grow NPôs as in previous methods the $AgNO_3$ with seeds $NaBH_4$ and the addition of sodium citrate. The only difference from previously mentioned methods is that PVP was used as a template. In photochemical synthesis, most of the works are mainly done on silver nanostructures with some modifications usually the addition of chemicals or the varying of the light source. In any photochemical synthesis usually, silver is somehow involved in one way or another.

2.6.4 Influence of Chemicals on Growth of the Structures

Dong and Zhou used the photochemical method to synthesize gold nanostructures [132]. The experiment was done under UV (300 nm) light and using a PEG-acetone mixture as a template also pre-synthesizing seeds of Au. The work reports that the speed of the reaction can be controlled via increasing the concentration of citric acid (increasing the concentration of the citric acid the reaction speed increases). The reaction resulted in near uniform spherical nanoparticles with sizes from 10 nm to 12 nm. They also report that by increasing polymerization degree the size of the nanoparticles decreases and the size of the nanoparticles increases by increasing the wavelength or irradiation.

The role of the pre-formed seeds. The addition of pre-formed gold seeds was added to the silver nitrate containing solution and then irradiated with UV light [132]. The result was the formation of an Au nanoparticle with an Ag shell. It is suggested that Au (seed) particles catalyze the reduction of Ag ions under the UV light leading to the formation of an Ag shell. Also synthesis of gold nanowires was modified by this group. First synthesis of Au nanowires was proposed by Esumi et al. [133] using UV light form a xenon lamp (200W) of 253.7nm and using $HAuCl_4$ and HTAC as a template. They report that only spherical particles obtained at low concentrations (1mmol dm-3) and only increasing the concentration up to 5 times the nanorods were obtained. The obtained nanorods of this group contained also nanoparticles and were varying in thickness and length. This method was improved by the previous group of Dong and Zhou [132]. They grew nanorods with more uniform size and length distributions. The novelty was the use of different solvents and mixtures of solvents. The mixture of DMF and water ratio can actually control and optimize the growth and the aspect ratio of gold nanorods. As a template in this synthesis CTAC was used. The solution contained DMF-CTAC-acetone mixture and the result of the synthesis highly depended on CTAC micelle. The explanation was that due to the change of solution polarity the CTAC micelle transforms from a spherical to a rod-like shape and thus leading to higher number of micelle aggregation. In this way molecules form almost perfect template for rod-like nanostructures. This statement was confirmed by changing the concentration of CTAC. It was found that at higher concentrations of CTAC the growth of nanorods is poor. This result could be explained by CTAC molecules blocking the pathway for the growth of nanorods. At optimal conditions the

aspect ratios from 50 to 150 were obtained. It was also found that longer exposure to the light time was favorable for the formation of the nanorods. The photochemical method is efficient and exciting since it can be controlled and always modified. Room temperature is always enough for the photochemical synthesis. Synthesis can be stopped at any moment of the synthesis process i.e light can be switched off. It is cheap and portable (depending on the size of the set-up) which is easy to install. On the other hand to run photochemical synthesis photo-sensitive chemicals are required which also limits the spectrum of materials that can be synthesized photochemically. The only problem is that the method is not very popular and very few articles are available in this topic.

2.7 Template -Assisted Synthesis of Nanoparticles

This method is widely used in nanosynthesis. Templates are usually used in order to achieve uniform structures and to avoid using high temperatures (in the liquid phase). In template-assisted synthesis the pre-synthesized template is usually in liquid phase and the molecules of the desired material are allowed to either settle down or make a chemical bond with the template (inside the template) thus usually it creates one dimensional nanostructures [134-136]. In most cases the templates are organic (like polymers) and the materials that are being synthesized are metallic or semiconducting [137]. In the case of template assisted synthesis in liquid phase the template could be: (a) dissolved in the liquid (water, acid or any organic liquid depending on the material) or (b) a solid prepared template (could be made from any material that is possible to nanostructurize or make desired voids or shapes). In the (a) procedure usually polymers are used. The desired structures are Ag, Au or alloy nanoparticles and in (a) usually polymers are dissolved and the metal precursor is added afterwards (for example $AgNO_3$). After stirring for some time in order to get the maximum interaction between the molecules the reducing agent is added for the formation of the nanostructures. The shape of the nanostructures is usually spherical but it also depends on the template. For instance, in the synthesis of silver nanowires only ethyleneglycol (EG) and silver nitrate are used [138]. The EG serves as both the reducing agent and the template. Also such polymers as dendrimers could be used as well, since they have a spherical shape and dendritic structure also most of them are soluble in water. The structure of the dendrimer is shown in Fig.2.5. As we can see the diameter of the dendrimer increases with the increase of the generation [139]. Dendrimers are

attractive because of the different functional groups that they have which can also be used in synthesis of hybrid materials dendrimer-nanoparticles for instance [140-142]. Linear polymers have an elongated structure and by using them as

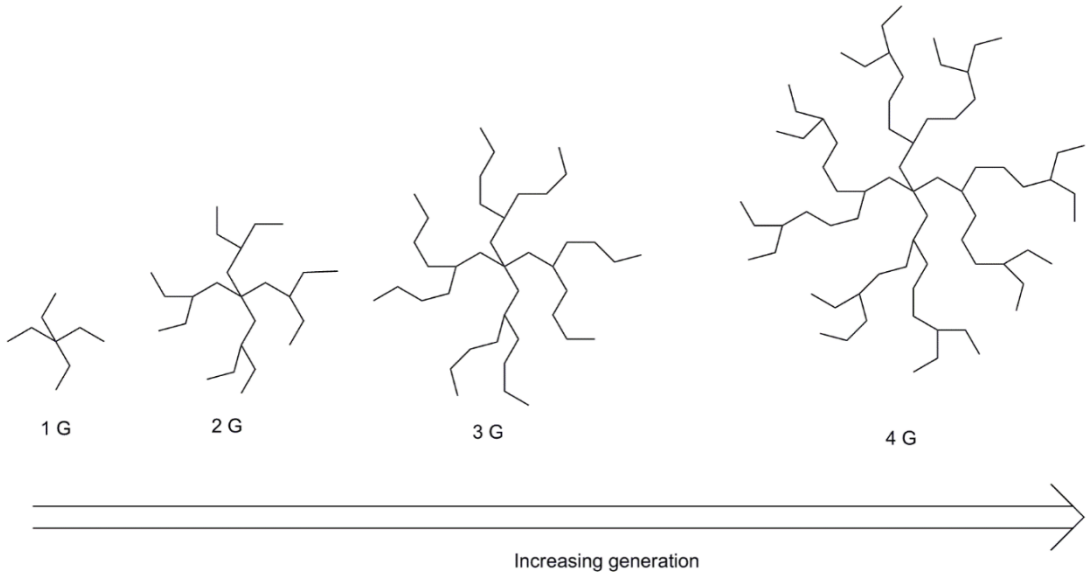

Figure.2.5 depicts structure of dendrimers: dendrimers have branched structure and different generations. With increasing generation dendrimers become more branched and their diameter also increases.

templates can limit the size and shape of metallic crystals by forming large nanoparticles. However, dendrimers have branches as depicted in Fig. 2.5 and nanoparticles can be synthesized either in between the branches Fig.2.6 or between the molecules of the dendrimers (if the concentration is high enough). Before the synthesis process using dendrimers we should pay attention to their unusual non-linear structure that can be easily chemically modified [143] this fact makes them attractive candidates for the template synthesis of nanoparticles. The only disadvantage is the high price. Important experiments were done using polymers in synthesis of gold, silver, platinum and palladium nanoparticles. Dendrimers have a branched structure thus they allow synthesis of very small nanoparticles (few nm) since the nanoparticle precursor (single molecule) can be incorporated between the branches of the dendrimer Fig. 2.6. After the reduction nanoparticles are limited molecule and

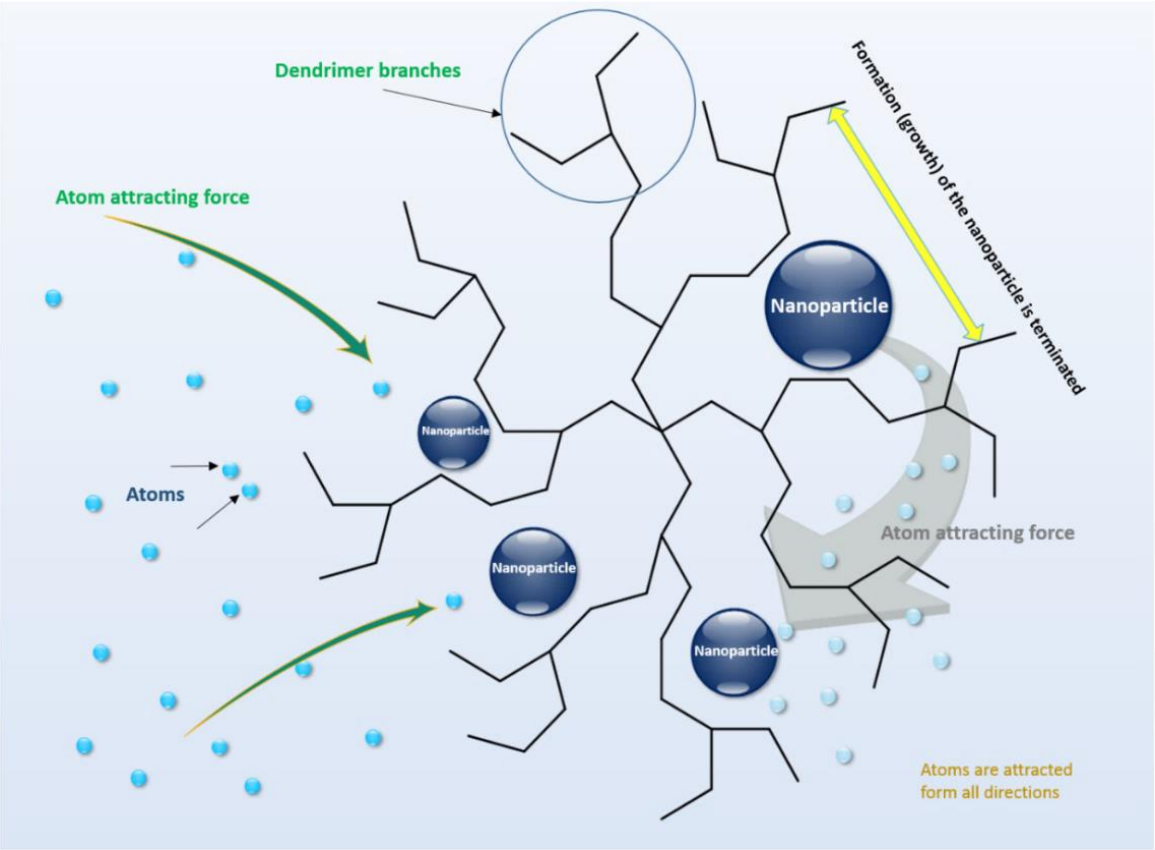

Figure. 2.6 one of the possible synthesis scenarios using dendrimers. The formation of the nanoparticles occurs between the dendrimer branches. When the growth occurs it is terminated by the dendrimer and this effect helps to template the nanoparticles and get the particular size depending on the concentration.

further growth is prevented. There are different types of dendrimers and they have different parameters and also can have various chemical groups attached. After the formation of the nanoparticles (in case of Ag and Au) the change of the solution color indicates the formation of the nanoparticles) the solution is centrifuged, washed and the structures are removed or if the template is attached to the material other chemical processes like etching might be involved. Thus some works in nanoparticle synthesis were performed using dendrimers that should be brought for consideration. One such works in synthesis of 1-2 nm gold nanoparticles using PAMAM type dendrimer was done by Kim et al [144]. The Au nanoparticles were spherical in shape and researchers proved that using a 4th generation dendrimer and higher it is possible to synthesize nanoparticles of less than 2 nm. And increasing the dendrimer generation basically no significant changes in size were observed. In such way also Pt and Ag nanoparticles were successfully synthesized with sizes ranging from 2.2 nm to 5.5 nm [145].

Reduction of $AgNO_3$ or $HAuCl_4$ with $NaBH_4$ is usually instant and can be expressed as:

$$AgNO_3 + NaBH_4 \longrightarrow Ag + 1/2H_2 + 1/2B_2H_6 + NaNO_3$$ Ó HÍ

$$4HAuCl_4 + 3NaBH_4 + 9H_2O \longrightarrow Au^0 + 3NaCl + 3H_3BO_3 + 13HCl + 6H_2$$ Ó HÍ

These reactions occur in liquid reducing metal precursors with strong reducing agents such as sodium borohydride. Adapted from ref [146]. Another process that exists in dendrimer encapsulated nanoparticle synthesis is the galvanic redox process. This process is the electron transfer between two metals in different oxidation states and refers to the electrochemical process. This process was used in Pd and Cu nanoparticle synthesis [147]. Using dendrimers usually small spherical particles can be obtained. This is a very powerful template since it can produce nanoparticles of sizes with less than 2 nm. One of the previously mentioned organic molecules is ethylene glycol and is also used in templated synthesis. EG with $AgNO_3$ produces Ag nanowires with different aspect ratios acting both as a template and a reducing agent. When $AgNO_3$ is dissolved in water it creates ions Fig.2.7. The ions float freely in a solvent and the molecules of EG hits them and mix. This is why usually such processes include stirring before the reaction starts. But in the case of EG and Ag it starts immediately and is not rapid like in the case of $NaBH_4$.

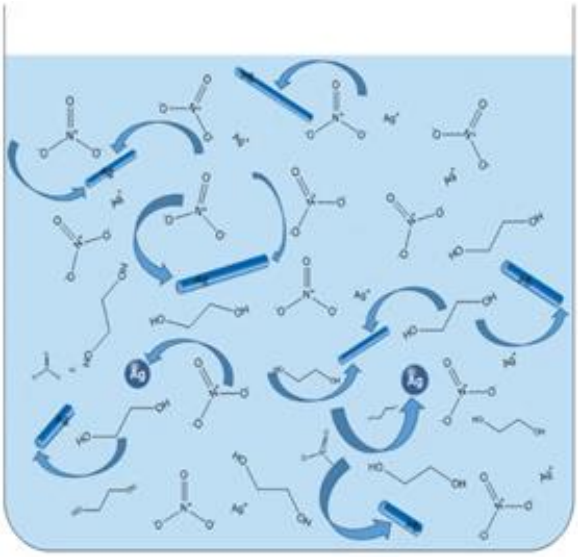

Figure.2.7 depicting the synthesis process of Ag in a liquid solution with the presence of ethylene glycol (EG) used both as a template and a reducing agent. As we can see after $AgNO_3$ was dissolved in the water (and time and then the reduction with EG) occurs.

After silver dissolved due to the reduction silver atoms start to attract each other thus forming subnanometer clusters. Later steps are the growth of the nanostructures but since they are in EG matrix they form linear structures such as nanowires Fig. 2.7. Also using a solid template is very popular in template assisted synthesis. The solid template is usually made of aluminum and called anodized aluminum oxide or AAO. AAO is usually a film with mutually parallel voids. AAO after its use as a template is dissolved and the nanowires collected by washing and centrifuging the supernatant Fig. 2.8. Using AAO template it is possible to grow a variety of vertically aligned materials including Si [148]. There are different types of AAO anodization and template preparation techniques and methods which can be found elsewhere [149].

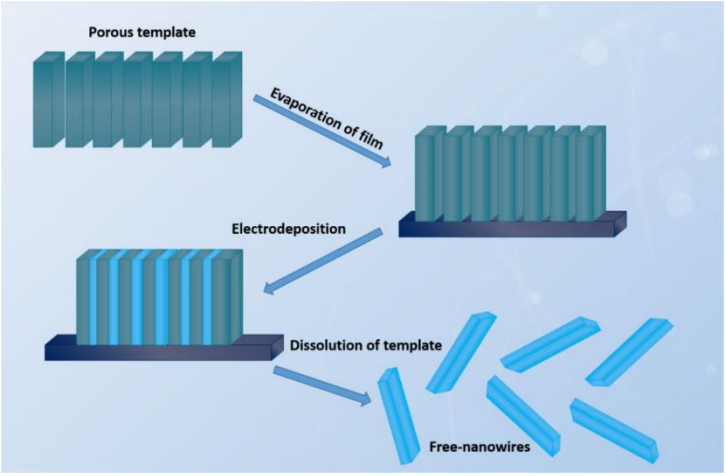

Figure. 2.8 porous Al template. First step includes evaporation of the film onto the template. Then electrodeposition and removal of the template leaving free nanowires.

Yang et al. used AAO in combination with the calcination process to synthesize Ag nanowires [150]. As indicated by SEM nanowires were vertically aligned with small defects that were Ag microparticles. Kim et al. synthesized Pd nanowires by pulsed electrodeposition [151]. Nanowires were of 500-700 nm in length and around 50 nm in thickness. The Pd nanowires were grown on $5cm^2$ area which can be considered as large. AAO can be used in synthesis of TiO_2 [152], Ni [153], carbon nanotubes [154], Au/Ni [155] however the products obtained by this template are usually in the shape of nanowires. The template-assisted synthesis method is efficient but only limited sizes and shapes like spherical particles or nanowires can be obtained in most cases. Also removal of the template and selection of the template creates extra complications for the process as such. The advantages of this method are that the structures obtained are very monodispersive, uniform in size and shape. This is a much desired quality for

industry and science. Template-assisted synthesis is also another very popular method for the nanostructure synthesis. The template if it is organic can drive the crystal growth in a particular way creating one or another shape of the crystal. This method has one disadvantage because it is not easy to remove the template after the synthesis. If the template is organic it also might interact with the synthesis product. If the template is not organic then another step of removing the template is required.

2.8 Control of End -Functionality of P3HT

Synthesis of conducting polymer has been a great interest for chemists for many years [156]. Electroconductive polymer or semiconducting polymer can be used in a variety of applications [157] since it has flexibility, solubility and a physical properties of a solid conductive material [158]. The properties of P3HT depend mostly on its end-functionality groups. In this work we are not going to synthesize or functionalize polymers. However, it is reasonable to briefly review the end-functionalization strategies of P3HT. There are two simple strategies for end-functionalization of P3HT: (1) Functionalization via Grignard metathesis polymerization and (2) use of functional Ni-based initiators.

2.8.1 Functionalization via Grignard M etathesis Polymerization (G RIM)

This strategy was reported first time in 2000 [159]. In this process using thiophene group Grignard McCullough-type polymerizations were successfully quenched. But this strategy was limited since it was applicable to only trimethylsilyl groups. McCullough suggested more efficient *in situ* functionalization strategy that involves GRIM polymerization quenching with different Grignard reagents [160, 161]. In this synthesis the end-functionalization is determined by Grignard reagent. Incorporation of additives like styrene and 1-pentene proven to control the end group composition [162]. Also Thelakkat and Lohwasser optimized the procedure and identified that excess of Grignard species and LiCl influence GRIM kinetics [163]. This improvement led into low polydispersity and perfect control of the end group of the polymer.

2.8.2 Functional Ni -Based Initiators

Ni-based initiators polymer synthesis strategy can provide almost perfect product with low polydispersity and controlled molecular weight [164, 165]. Specially designed Ni-based initiators can give a variety of P3HT polymers with different end groups like: amino, ethynyl, carboxylic acid or phosphonate [163, 166-168]. Also a concept for Ni-based external initiators led to a synthesis of P3HTs with different end-functional

groups like: pyridines, thiols, and phenols [169]. This approach also allows synthesizing complicated polymeric architecture. The disadvantage is that traces of Ni impurity can disturb the desired polymer chain

2.8.3 Organic Molecules and the Morphologies of Thin Films

Synthesizing the polymer or adding specific functional groups to its end is still half way to the application. The main question is: what will we do after the desired polymer is synthesized? We will answer this question in the next subchapters. The synthesis or structuration methods sometimes limit the morphology of the nano or microstructures [170]. Organic molecules like polymers play an important part in the synthesis of nanomaterials [171]. Polymers can be synthesized for a variety of purposes like photovoltaics[172] or sensors [173]. The synthesis of polymers is beyond the scope of this work. However, a brief introduction on polymer synthesis will be reviewed and discussed. Special attention is given to morphological variations of the structure of polymers on the nanoscale.

2.8.4 The Importance of Polymer Morphology

The present work focuses on a few types of polymers which are semiconductive. Semiconductive polymers have a very wide range of applications as mentioned above from solar cells to light emmiting diodes or LEDs. The most popular are thiophene type polymer and the PCBM monomer mixture. They are relatively cheap and used as a "Playground" for researchers in order to develop concepts about processes happening on a nanoscale. Thiophene type polymers can be dissolved in a variety of solvents at room temperature which gives the flexibility required for the research.

2.9 Morphology of Polymers and Influence on Organic Solar Cells

Progress in organic solar cells led to the development of novel nanostructuration methods of the polymer layers [174-177]. As has been demonstrated the efficiency of the polymer solar cell strongly depends on the materials and nanomorphology of the polymer layers [178]. For a better understanding of the topic first donor acceptor materials should be introduced. The most efficient proven to be P3HT/PCBM and PTB7/PCBM mixture layers [179]. The first layer P3HT/PCBM where P3HT-RR corresponds to Poly(3-hexylthiophene-2,5-diyl) regioregular (RR) which is a donor and PCBM stands for [6,6]-Phenyl C butyric acid methyl ester where C- is a fullerene which can be usually C61 or C71 and this derivative is an acceptor in an organic solar cell film. PTB7 is poly[4,8-bis[(2-ethylhexyl)oxy]benzo[1,2-b:4,5-b Nj] dithiophene-2,6-

diyl][3-þ u o-2-[(2-ethylhexyl)carbonyl]thieno[3,4-b]thiophenediyl] and is one of the most efficient low bandbap polymers for the photovoltaics. PCBM acceptor contains benzene ring and fullerene Fig.2.9. atoms in the fullerene.

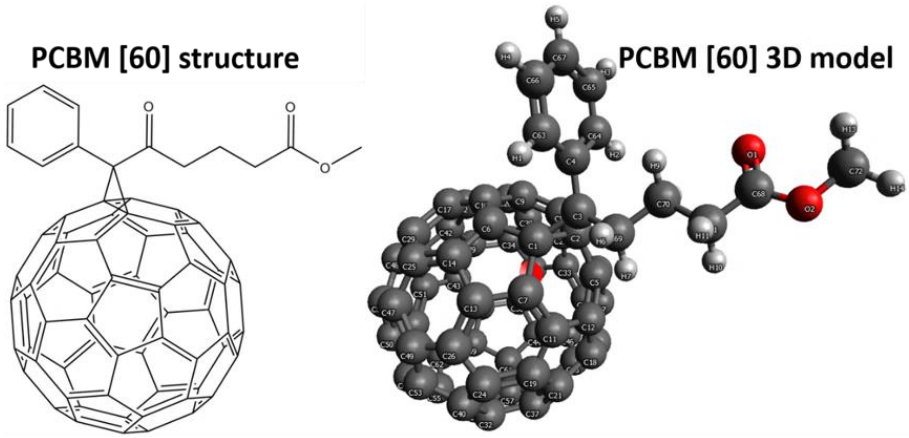

Figure 2.9 structural formula of PC61BM and 3D model.

The most popular type of PCBM is $PC_{61}BM$ and $PC_{[70]}BM$. The difference between these two molecules is the amount of carbon atoms $PC_{60}BM$ contains 60 carbon and $PC_{[70]}BM$ contains 70 carbon atoms Fig. 2.10. The second molecule reported to be more efficient in organic solar cells (C70). PCBM makes one of the best acceptor materials due to its solubility in organic solvents. This is very important feature in order to achieve printable and thin film solar cells.

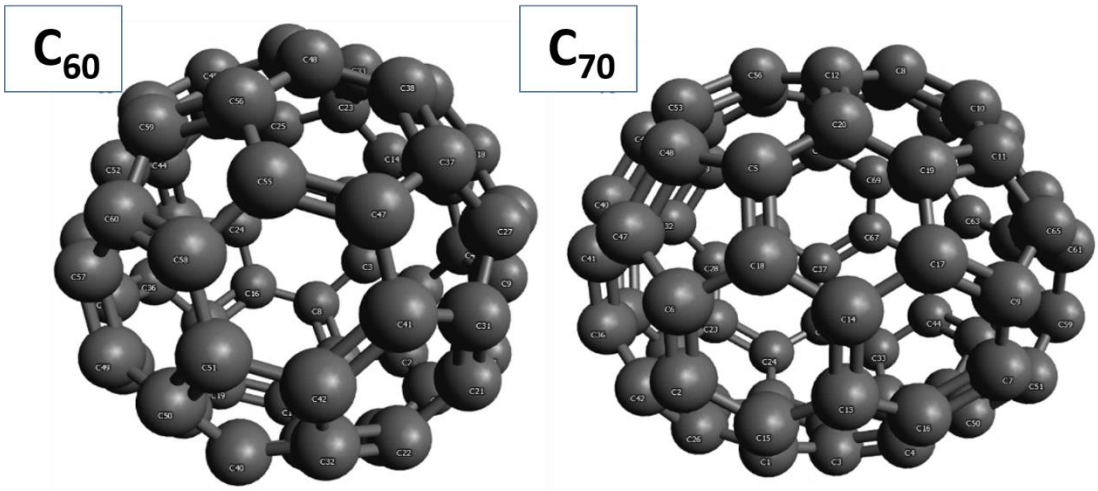

Figure. 2.10 depicts 3D models of fullerenes of two different kinds: C60 in the left and C70 in the right. These molecules define the number on PCBM molecule.

PCBM and its derivatives are usually a necessary ingredient for the organic photovoltaic devices which show very high power conversion efficiencies [180-182].

2.9.1 P3HT/PCBM -Based Solar Cells

Another very important and probably most popular semiconducting polymer used in flexible solar cell fabrication is the P3HT [177]. This polymer has good donor properties and is widely used for solar cell fabrication. The structural formula of P3HT and the 3D model are depicted in Fig. 2.11. It is reported that P3HT in organic solar cells makes a p-type bonding thus creating a particular nanomorphology of the film [172, 183]. This type of nanomorphology usually characterized by AFM. Nanomorphology has a great influence on the performance of the solar cells [184, 185]. Such AFM investigations were performed by Villers et al [186]. The work included nanomorphology control in P3HT/PCBM films. They show that PCBM creates domains in the film thus greatly influencing the morphology of the film. Keawprajak et al. studied the influence of solvent on thin P3HT/PCBM film [187].

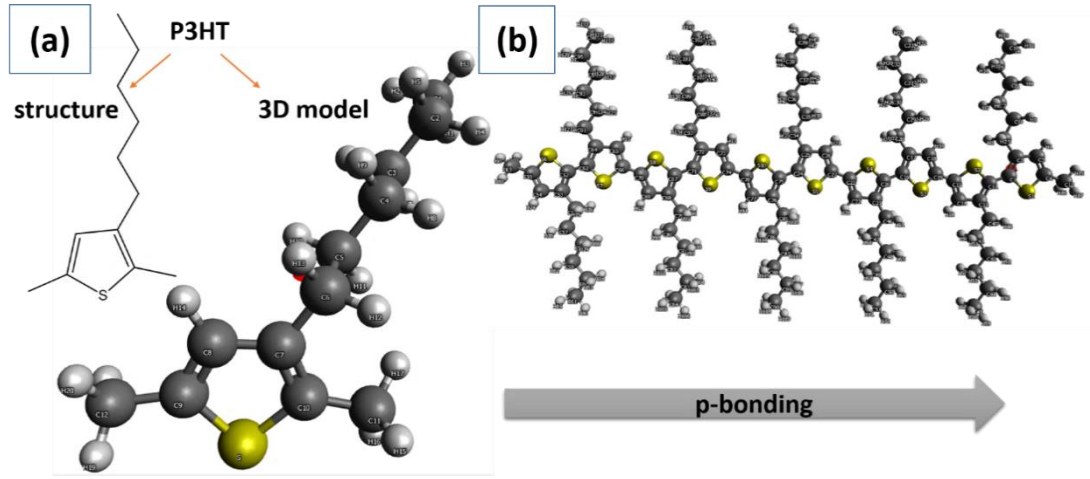

Figure. 2.11 depicts the P3HT semiconducting polymer. (a) the structural molecule and the 3D model of the P3HT and (b) the stacking of the P3HT molecules by p-bonding within the films reported by some works.

They improved solar cell PCE by 20% using TCB and temperature treatment. The roughness of the films was influenced both by solvent and temperature treatment. Lowest roughness was achieved by applying 180^0 C temperature and lowest TCB concentration of 12mg/ml. It is important to mention that the A F M s c a n a r e a w a s which is relatively high for this type of scan. Another report by Chirvase et al. has also shown the influence of nanomorphology upon the performance of the photovoltaic device [188]. Different amounts of PCBM were added to the P3HT/PCBM mixture. An AFM scan was performed at different amounts of PCBM and revealed the formation of nanohills when the concentration was 50%. Also the device showed best characteristics at 50% of PCBM.

2.9.2 Influence of Temperature on Polymer Morphology

The influence of temperature on polymer films showed also morphological changes which led to the structural changes inside that could either increase or decrease the device performance [189]. Shi et al. incorporated nematic liquid crystal into the P3HT/PCBM matrix and improved the PCE [175]. Increasing the amount of liquid crystal AFM images showed changes in nanomorphology. At weight amount 3% the textures could be barely seen but increasing it to 6% it was more obvious. When the amount of liquid crystal was increased to up to 10% the textures were clearly seen and the upper and lower parts of the film were observed which indicated specific orientation of the P3HT/PCBM and liquid crystal. However, it was difficult to analyze the micrographs since they were not analyzed in detail. It was difficult to answer the question whether it was the P3HT or the PCBM or the temperature that was influencing the morphological changes.

2.9.3 Structural Changes of the P3HT

Grigorian et al. made an investigation on the structural properties of the P3HT [176]. The work revealed that drop-cast P3HT films were highly crystalline and underwent minor changes during temperature treatment. On the contrary films deposited by spin-coating exhibited less crystallinity and changed much more under temperature treatment. It is important to mention that for the investigation Gazing Incidence X-ray diffraction was used (GID). They concluded that P3HT underwent structural changes under temperature treatment and that those changes were reversible. Also they concluded that at high temperatures the crystallite sizes and distances interstacking spacings, crystalline packings are influenced as well. Nicho et al. studied P3HT and different organic molecules [177]. The AFM was used for the morphological charactersations. Researchers showed that by varying the amount of organic molecules it is possible to control the nanomorphology of the P3HT films.

2.9.4 P3HT Mixture with other Polymers

Mixing P3HT with other polymers can give a different morphology. Thus using polystyrene (PS) and P3HT mixture in toluene to make thin films by spin-coating revealed morphology changes upon the variation of the amount of PS. 80:20 ratio led to the formation of spots with diameter ranging from a few hundreds of nm to up to a few microns [177]. 60:40 led to the wider spots with similar sizes as that of 80:20 ratios. The most interesting was 0.5:95 by weight which led to a complete

nanostructurisation of the features on the film (nano-island formation). The same experiment was done using polymethylmetacrilate (PMMA). Changing the amount of the secondary organic molecule researchers demonstrated a relatively high control of the nanomorphology of the P3HT film using toluene as a solvent. Saini et al. demonstrated that the influence on the P3HT could be done by using carbon nanotubes [190]. It was found that multi-walled carbon nanotubes can be dispersed uniformly within the P3HT and as a matter of fact polymer wrapped around the tubes. NMR analysis indicated a chemical interaction between the polymer and the tubes. Lu et al. investigated P3HT/PCBM [60 and 70] morphologies via optical techniques [180]. They fabricated solar cells with efficiencies of around 5%. The finding of this work was that annealing helped to improve the PCE of the device. Increasing the annealing temperature PCBM was forming clusters which were removed by addition of Al. The temperature range was from 100 C to 280 C. By increasing the temperature PCBM clusters were increasing in numbers at 180 C. The investigation of the morphology was conducted mainly via an optical microscope which did not show the nanomorphology. However, microfeatures greatly depend on the nanofeatures.

2.9.5 Solvent Influence on M orphology

Chang et al. also studied the effects on the solvent residues in the P3HT/PCBM films also using optical microscopy [181]. They showed that casting the solvent has an influence on the morphology of the films. They also showed that regardless of the solvent PCBM agglomerates when heated up have an influence on the solar cell parameters. Liao et al. used different solvent annealing and investigated the effects on the morphology of the P3HT/PCBM films [182]. Researchers used non-solvent, bad and good solvents to show the influence on the morphology. PCBM and P3HT molecules were arranging differently within the film after the vapor treatment which was affecting the device parameters.

2.9.6 Annealing Un der Solvent Vapours

Another similar work was performed by Verploegen et al. [183]. This work included an investigation of solvent vapors on the P3HT/$PC_{60}BM$ morphology. They found that THF can induce crystallinity in PCBM. THF and chloroform vapor annealing resulted in the swelling of the P3HT layers stacking grains which leads to morphological changes and can improve device performance. Chen et al. used the annealing method to investigate the performance on the devices based on

P3HT/PCBM [172]. All of the methods of polymer morphology control mentioned above are either solvent and solvent mixture based or temperature based. The P3HT/PCBM system is usually the most investigated however another increasingly popular system is the PTB7/PCBM Fig.2.12. This donor-acceptor system can give higher efficiencies of the devices and has a bright future in the area of flexible photovoltaics. However, the control of this type of polymer seems to be the same as controlling any polymer morphology since the same conditions can be applied to the PTB7 and the morphology change can improve the device efficiency.

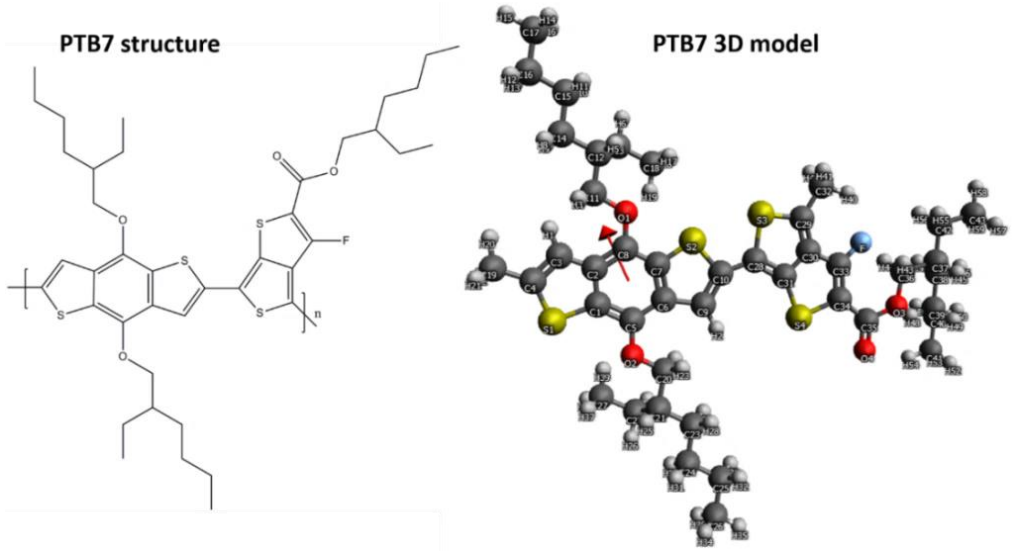

Figure. 2.12 PTB7 structural formula and 3D model in the right.

Guo et al. demonstrated such PTB7 property by preparing films and the influence of the solvents such as chlorobenzene, 1,2-dichlorobenzene, and 1,2,4-trichlorobenzene were investigated [191]. The used polymer had 40% of fluorinated monomers and 1,8-diiodooctane can improve the performance and influence the morphology which are correlated. The films that were made using chlorobenzene had the smallest domains while the DIO influences the PCBM and not the PTB7 which also influences the whole PCE of the device. He et al. fabricated PTB7/$PC_{[70]}BM$ inverted solar cell with an efficiency of 9.2% which is greatly higher than most polymer based solar cells [192]. This article proposes the trend towards 10% which actually can be commercialized. However, currently there are not many works reporting PTB7 morphology manipulation since most of the works are aiming at creating solar cell and increasing the efficiency. Another work by Yanagidate et al. was also creating the PTB7/ $PC_{[70]}BM$ device that had a LiF buffer layer which helped to improve the PCE [193]. The morphologies characterized by the AFM showed that the device with greater

efficiency had smaller nanofeatures however the roughness measurements were not provided. The P3HT/ $PC_{[70]}BM$ and PTB7/ $PC_{[70]}BM$ systems are the most popular and used for the organic solar cell prototype in the laboratory. Depending on the conditions applied polymers can arrange in a particular way which will cause the solar cell efficiency. The main problem is the control of the arrangement of the polymers which still remains a challenge.

2.10 Summary

This chapter gave the introduction to the existing synthesis methods of the nanomaterials. Most important techniques and strategies were reviewed and analyzed. Existing techniques require expensive equipment (VLS or CVD) or high temperatures and/or dagerous chemicals (hydrothermal method). Special attention is given to the photochemical synthesis. In most cases photochemical synthesis can be performed with light-responsive materials or chemicals. Unfortunately not many works has been done in this direction and clear gap can be filled with the light-induced synthesis proposed in this work. Photochemical method is limited to the Ag or Au. Or can be with plasmon-related mnaterials. If the light is not absorbed by the material then the material cannot be affected by the light. Other synthesis methods are well investigated and high precision is achieved over the years using them by a variety of scientists over the World. This fact puts light-related synthesis method in a shadow as less efficient and undeveloped. Photochemical synthesis is the smallest subchapter in the literature review and the method requires an improvement. Also existing nanostructuration methods for the polymers was reviewed and analyzed. Surface morphology can influence overall efficiency of the solar cell and is very important for the future organic photovoltaics. Most popular semiconductive polymers were considered and the strategies of improving their morphology was reviewed. The most common strategies of changing the polymer film morphology is the treatment of the polymer film with solvent vapours or heating it up called annealing. Polymer surface morphology variation is really limited due to the polymer chemistry and is time consuming.

Chapter 3 Experimental Methods

In this chapter experimental methods such as the experiment set-up preparation, synthesis procedure, sample preparation and characterization will be described. Characterization methods and techniques are introduced and described.

3.1 Raw Chemicals

For the synthesis of nanoparticles and nanostructures the raw materials were used: oleic acid ($C_{18}H_{34}O_2$), nitric acid 70% (HNO_3), chloroauric ($HAuCl_4$), P3HT Poly(3-hexylthiophene-2,5-diyl) regioregular 1g, $PC_{[70]}BM$ [6,6]-Phenyl C71 butyric acid methyl ester mixture of isomers 99% 500mg, chloroform 2l, dimethylformamide 500ml, tetrahydrofuran 2l, dimethylsulfoxide 1l, xylene 1l, ethanol, ethanol anhydrous. Silver nitrate, sodium hydroxide, cadmium acetate dihydrate, sodium borohydride (powder), tri-sodium citrate dihydrate, cadmium acetate dihydrate. All chemicals were purchased from Sigma-Aldrich UK. Substrates: silicon wafers 7X5 and mica (for AFM) were purchased from Agar Scientific. For the TEM investigation copper grids formware were also purchased form Agar Scientific. PPI-G4-32 dendrimer from SyMO-Chem.

3.2 Procedure for Synthesis

3.2.1 Synthesis of Gold Nanoparticles

For the gold nanotriangle synthesis oleic acid, nitric acid and chloroauric acids were used. Step1: Chloroauric acid was weighted to have 1mmol and added to the 50ml vial. Step2: 0.1ml of concentrated (70%) nitric acid was added to the vial with chloroauric acid. Step3: Oleic acid was added to the vial(50ml) and shook manually. The solution was left for 24 hours without further stirring. After 24 hours the bright yellow precipitate removed and deposited via drop-coating on the silicon wafer for the ESEM without further procedures. Schematic depiction of the experiment is depicted in Fig.3.1.

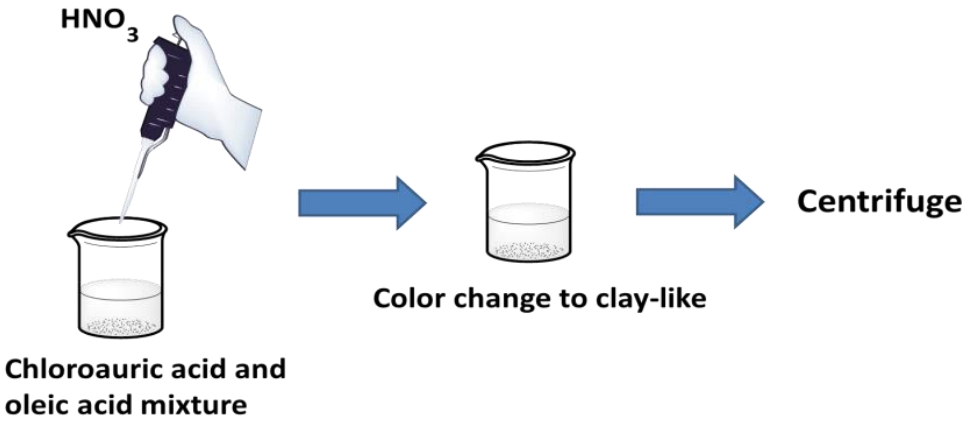

Figure 3.1 shows the experimental set-up scheme. In the mixture of chloroauric and oleic acids concentrated nitric acid is injected using a micropitette. Then after some time when the color of the liquid changes to bright clay-like the nanoparticles are formed. The last step is centrifuge and the extraction of gold nanoparticles for the characterization.

The extraction of nanoparticles was performed using ethanol and distilled water. The solution turned to be clay-colored and was not liquid anymore. It looked like a solid soap. First ethanol was used to dissolve the particles. After dissolving the particles the solution was centrifuged two times in ethanol and then 3 times in water. For easier sample preparation ethanol can be used as a solvent.

3.2.2 Synthesis of CdS Quantum Dots

Cadmium acetate dihydrate ($Cd(CH_3CO_2)_2$) 1mmol was added to the 20ml vial along with 15ml of distilled water and 1mmol of PPI(SyMo-Chem) type 4th generation dendrimer (poly(propylene imine))) containing NH_2 groups. The mixture was stirred overnight at 200 rpm stirring speed using a magnetic 1cm bar. The next step was the addition of sodium sulfide (Na_2S). For the AFM characterization, the solution was spin-coated at 2500 rpm for 60s on a silicon wafer (AgarScientific).

3.2.2.1 Preparation Procedure of CdS Quantum Dots

The synthesis of CdS was performed under nitrogen atmosphere and at room temperature. Two three neck chemical glasses were used to prepare the components for the synthesis. Rubber caps were used to cover all the 3 necks first. Then in two of the rubber caps sterile syringe needles were inserted to ensure the nitrogen circulation. The middle neck was connected to the nitrogen bottle fig.3.2 After the chemicals were dissolved the Na_2S solution was injected from step1 to step2 using a syringe and

elongated needle. After the solution turned from transparent to yellowish it indicates that CdS quantum dots were formed.

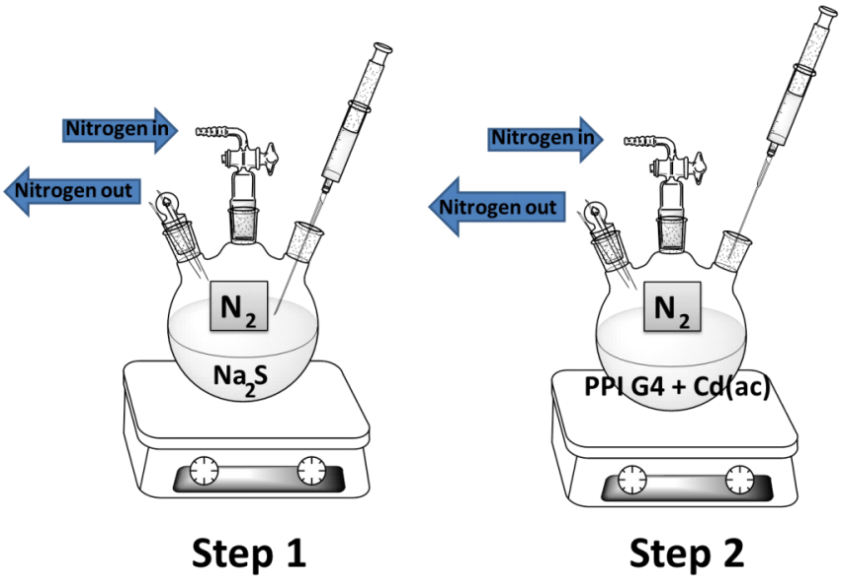

Figure 3.2 depicts synthesis of ordered CdS quantum dots using a PPI type dendrimer. At first all the chemicals are dissolved separately in a solvent. And the nitrogen flow is provided to both mixtures. The mixture containing sodium sulfide is taken from the solution step 1 and injected into the solution containing cadmium precusrsor and the dendrimer step 2.

3.3 Experiment Set-up for Synthesis of ZnO, Ag, Ag-Au Nanostructures

In this subchaper we will describe the light-induced synthesis set-up preparation and procedure used. Light-induced synthesis was performed at room temperature for ZnO, Ag, Ag-Au and nanostructuration of the polymer films P3HT/ $PC_{[70]}BM$ and PTB7/ $PC_{[70]}BM$.

3.3.1 Experimental Set-up for Light-Induced Synthesis

For all these materials (ZnO, Ag and Ag-Au) the same experimental set-up was used. This consisted of a laptop, a microcontroller, LEDs, prepared solutions and a synthesis chamber. The detailed experiment set up is shown in Fig.3.3.

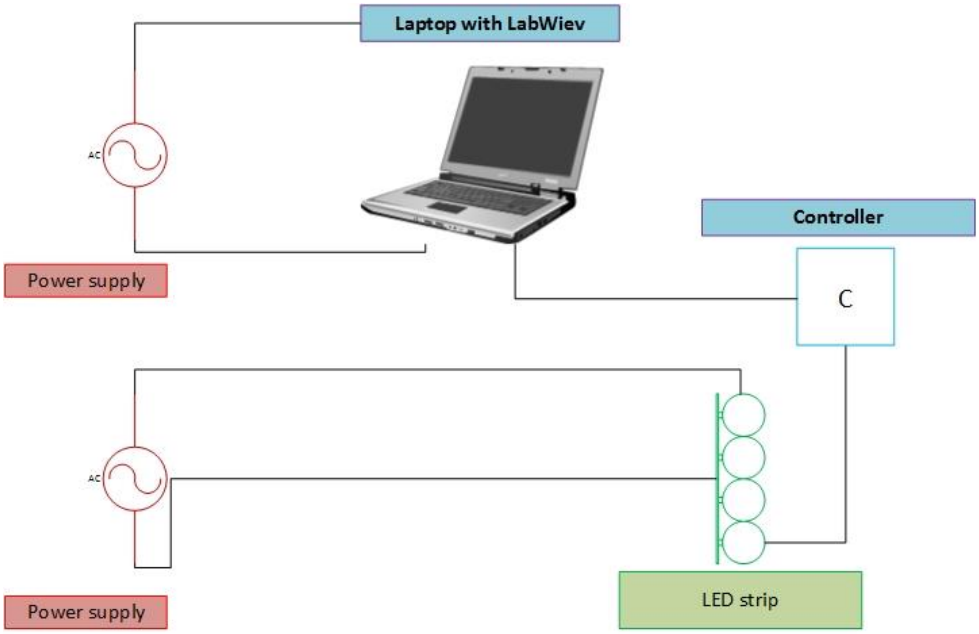

Figure.3.3 depicts the setup of the experiment. The main components are the LED strip and the controller with a laptop. The controller was programmed from the laptop and then the LED strip was placed into the synthesis chamber with the chemical solution.

The control of the LED sequences was programmed using LabWiev Software and transmitted from a laptop to the controller and then to the LED. The controller was a National Instruments USB 6008 driving the LEDs via solid state relays. The key point of this experiment was to control the energy (light) portions to the samples. This set-up allowed great light-induced synthesis control and time-dependent energy portions from different parts of the optical spectrum. Also it was possible to control the cycle number which precisely controlled the synthesis time. The synthesis chamber was simply black box with aluminum foil inside to reflect the visible light. The distance between the light source (LED) and the sample was always 15cm.

3.3.2 Procedure for Light -Induced Synthesis of ZnO

Zinc acetate dihydrate ($Zn(O_2CCH_3)_2(H_2O)_2$) was dissolved with different molar ratios (1mmol, 2mmol, 3.2mmol) in distilled water (20ml vial 15ml of water) with the addition of of 1ml of ethanol. Then from the stock solution 1ml of sodium hydroxide (NaOH) was added (2mmol/ml). The vial was immediaty placed into the light chamber. The light sequence was chosen to be as shown in Tab.3.1. All the chemicals were purchased from sigma Aldrich. For Ag and Ag-Au synthesis these sequences were slightly modified (RGB and green-red) and for the polymers only red and blue lights were used. Photoinduced synthesis and nanostructuring were carried out for

12hours in the synthesis chamber. RGB-code was 1s red, 1s green and then 1s blue. Then the cycle was repeated.

Table.3.1 the light sequence code for the ZnO synthesis experiment.

Title	Wavelength (nm)	Wavelength (nm)	Wavelength (nm)	Wavelength (nm)	Wavelength (nm)	Wavelength (nm)	Time
Code1	634 (red)	518 (green)	634 (red)	518 (green)	634 (red)	Off	12h
Code2	634 (red)	461 (blue)	634 (red)	461 (blue)	634 (red)	Off	12h
Code3	518 (green)	461 (blue)	518 (green)	461 (blue)	518 (green)	Off	12h
Code4	518 and 461	461 (blue)	Off	518 (green)	634 and 518	518	12h
Time	10 seconds	30 seconds	25 seconds	10 seconds	25 seconds	10 seconds	Repeating

3.3.3 Specifics of the Light-Induced Synthesis

The light-induced synthesis set-up and conditions were the same for all the materials ZnO, Ag, Ag-Au and nanostructuration of the polymers. The specifics of the synthesis revealed the importance of every small and non-significant move and condition. Such as importance whether the experimentalist will inject or pour sodium hydroxide into zinc acetate or the other way around. The results can change dramatically leading to results with a great bias. Also if the vials or chemicals used are not pure enough this would lead to a change in shape and or size of the final product.

LED light.During the synthesis a LED light must be switched on all the time. Before the chemicals are mixed a LED light must be on and also during the mixture of the chemicals. It is also recomended to do the synthesis in the dark area where the daylight cannot reach the samples (because of UV). For the synthesis in dark it is also recommended to wrap the vials or beakers in aluminium foil to avoid any light reaching the chemicals. Also when light is shinning through the bottom of the vial it does not influence results Fig.3.4. The influencial factor is stirring or shaking. No magnetic stirrers or shakers should be used. This helps to assemble the hierarchical nanostructure. For better analysis the light wavelenght should be measured and the spectrum obtained. Since every light wave (color) has a different energy it is very important to know which energy portion (higher or lower) influences the growth. The LED wavelength of light was characterized using an OceanOptics USB4000 optical bench spectrometer calibrated from 300nm to 800nm and used with SpectraSuite software.

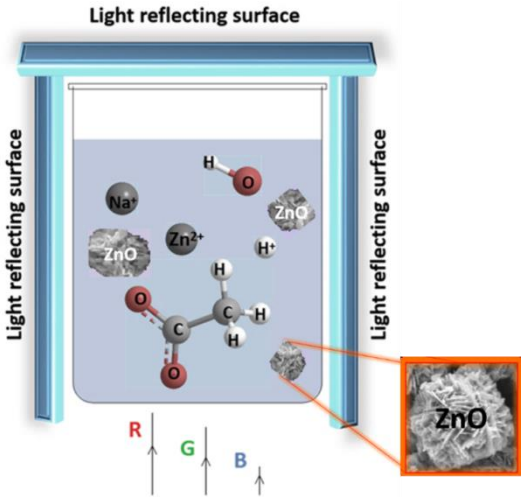

Figure.3.4 shows schematic set up of the ZnO light induced synthesis at room temperature. The vial or glass beaker is surrounded with light reflecting surfaces and the light is shining from the bottom.

3.4 Procedure of the Synthesis of Ag and Ag-Au Nanostructures

Silver nitrate ($AgNO_3$) was prepared with a concentration of 1mmol/ml in a 20ml vial (15ml of the solution) in distilled water. The second step was the addition of trisodium citrate ($Na_3C_6H_5O_7$) with the same concentration (1mmol/ml) of 1ml and placing the solution into the light chamber without stirring. To produce Ag-Au nanoalloy the addition of chloroauric acid with the molar ratio to make 50:50 (50% of Ag ($AgNO_3$)and 50% of Au ($HauCl_4$)) was prepared into a 20ml vial and placed into the light chamber for 12 hours. The samples were prepared for the SEM investigation without further washing or centrifuging by drop-casting and drying then at 40^0 C temperature for 4-5hours.

3.5 Polymer M orphologies

A morphological structure change experiment was performed using semiconductive polymers and a LED light. The experimental set-up described in subchapers 3.4 ï 3.6. The morphological change was performed with polymers in the chloroform at room temperature and using a LED lights of two wavelengths red (633nm) and blue (461nm).

3.5.1 Light -Induced Morphology M anipulation of PTB7/ $PC_{[70]}BM$ and P3HT/ $PC_{[70]}BM$

The P3HT, PTB7 and $PC_{[70]}BM$ were purchased from Sigma-Aldrich and used without further purification. For the experiment two types of solutions were prepared: P3HT/ $PC_{[70]}BM$ and PTB7/ $PC_{[70]}BM$. The molar ratio was chosen to be 1:1. For the solvent-

based experiment only the P3HT/$PC_{[70]}BM$ system was used. For the light-induced nanostructuration experiment two systems were used: P3HT/$PC_{[70]}BM$ and PTB7/$PC_{[70]}BM$. All the solutions were in chloroform ($CHCl_3$). After dissolving the polymers the samples were placed into the light chamber without stirring and left for 12 hours. After the light chamber the solutions were spin coated on a silicon wafer and characterized using AFM.

3.5.2 Specifics of Polymer Morphology Light -Induced Approach

This experiment that proven light can influence the morphology of the polymer films has few important details that are worth mentioning. First of all chloroform was chosen since it is the best solvent for these polymers. Secondly the concentration plays an important role. The concentration as it was mentioned in 3.10 was 1:1 molar ratio of both polymers. If the ratio will be 1:10 then the solution turns too dark (it is dark brown in color) and the light cannot penetrate through the sample. Also chloroform evaporizes very fast and vials should be closed immediately after adding a polymer. In this experiment it is not important whether the chloroform is added first into the vial or the polymer. Also a polymer mixture should not be stirred while under a LED light. Stirring can greatly influence the overall result.

3.6 Characterisation E quipment

In this subchapter the equipment used for the characterisation of the materials will be described. The parameters of the equipment and the working principle will be analyzed. Important features like the advantages of each method will be emphasized.

3.6.1 High Resolution Transmission E lectron Microscopy (HRTEM) and High -Angle Annular Dark -Field Imaging (HAADF)

Transmission electron microscopy (TEM) measurements were carried out on a (high resolution) TEM (TECNAI Biotwin, FEI Ltd. and JEM-2110F, JEOL) operated at 100 kV and 200 kV, respectively. Prior to the TEM measurements, a solution with nanoparticles was drop-coated on carbon coated copper grids (400 mesh, AGAR Scientific) using a solid substrate support. The HAADF was intergrated and conducted for the duration with the HRTEM scan in STEM mode.

3.6.2 HRTEM Working Principle

The Transmission Electron Microscope can provide a better resolution than any optical microscope in existence and zoom into the lattice of the crystal. In Fig.3.3 The TEM working principle is depicted. First the source of the electrons called the electron gun Ăshootsñ the electrons to the sample. The electrons then scatter and fly in many directions and this is where the magnetic lense comes to the aid. Magnetic lense can focus the electrons via the magnetic field. The magnetic lense is basically an electromagnet.

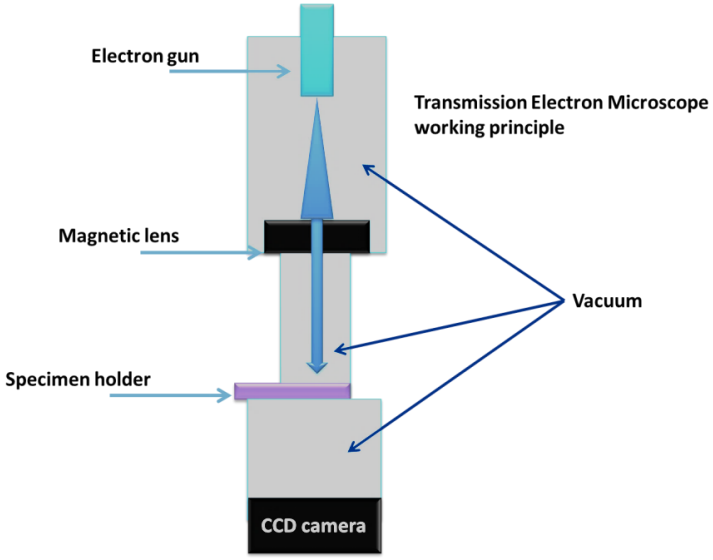

Figure 3.3 depicts schematics of the TEM working principle. The electron gun shoots the electrons through the magnetic lense which focuses the beam. Then the beam goes through the sample. Normally the electron beam falls on the fluorescent screen showing the result. But today electron microscopes are equipped with CCD cameras which helps to improve the characterization.

The TEM itself has a chamber or camera (made of steel) and it contains a high vacuum. When electrons pass through the sample they cannot get through thick areas of the sample. For instance metal nanoparticles would stop some electrons creating a shadow which would be visible on the CCD camera (which is connected to the PC).

3.6.3 HAADF Mode

The dark field mode of the HAADF can show the areas which are reflecting the electrons. It is a HRTEM mode and the image of an object (a nanoparticle for example) appears bright while on a dark background. The bright areas shows the reflected electrons and can help determine whether it is an organic soft material (if the operator is not sure). In the HAADF mode the sample can be titled to collect back-diffracted electrons called Bragg reflections. This method is also used in studying lattice defects.

3.7 Characterization using Environmental Scanning Electron Microscope

The ESEM characterization has been carried out using a JEOL WINSEM JSM-6400 at a 20kV accelerating voltage as well as a Phillips FEI XL30 FEG-ESEM with various accelerating voltages. Incorporated into the ESEM is an EDX analyzer supplied by Oxford Instruments. EDX scans have been carried out on different parts of the sample in order to confirm the elemental analysis of the structures.

3.7.1 Scanning Electron Microscope (SEM) Working Principle

The SEM is an elecron microscope which uses electrons to hit the sample and then the reflected electrons hitting the detector create an image Fig. 3.4. The electron microscope is used to study both the metallic and polymeric structures. It does not go through the sample like in the TEM scan. The SEM can be compared to an optical microscope apart from the fact that it uses electrons instead of light. Electrons behave like waves (due to the particle-wave duality) and at high energies have low wavelengths. The SEM image is produced due to low energy secondary electrons. The more electrons that are reflected the brighter the image is. Electrons that go into the depth of the sample (for example into the void or pit of the structure) are usually absorbed and not reflected into the detector. The best modern SEM can achieve a resolution of less than a 1nm.

3.7.2 Environmental Scanning Electron Microscopy (ESEM)

The Environmental Scanning Electron microscope is a Scanning Electrone Microscope that is designed for wet or biological samples. The specimen for the ESEM does not have to necessarily be coated. The ESEM allows a more detailed investigation on biofilms and is mostly widely used in biosciences

.

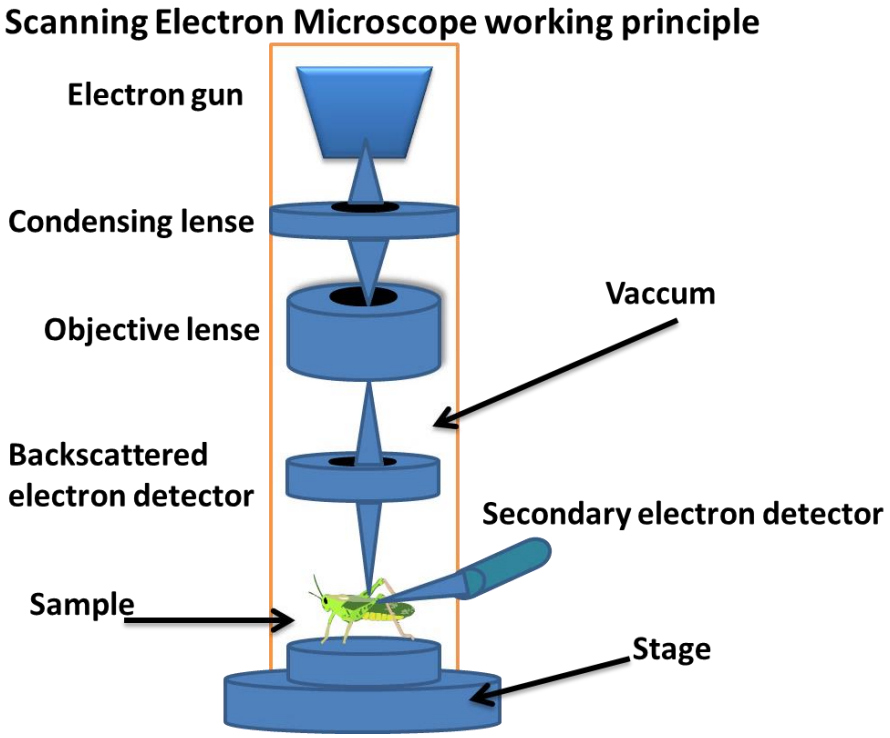

Figure 3.4 depicts the working principle of SEM. The first electron gun creates a beam of electrons which are focused by magnetic lenses. Then after being focused they hit the sample and get reflected from it into the detector which then creates an image. The whole process happens in a high vaccum.

3.7.3 Dispersive X-ray Spectroscopy (EDX)

The EDX is usually an option in SEM and can be used to determine elements in the material. It shows which chemical elements are on the sample or the composition of the sample. When the electron is released from the material it creates a hole and another electron with the higher energy fills the hole releasing energy in the form of an x-ray. Secondary electrons make every element emit a characteristic x-ray (a specific x-ray with different energy portions). The x-ray signal can be separated by a silicon-lithium detector then the signal is amplified and analyzed.

3.8 Atomic Force Microscope (AFM)

An Atomic force microscope (Dimension 3100a Nanoscope, Veeco Instruments Inc.) was used to image the fabricated nanofibers and polymer thin films. The imaging of the samples was conducted in tapping mode using silicon nitride cantilevers (Bruker AFM Probes) with a resonance frequency of about 330 kHz, a spring constant of 45 N/m and a tip radius of less than 10 nm.

3.8.1 AFM Working Principle (contact mode)

The Atomic Force Microscope (AFM) was used in the present work to determine the surface morphology or texture of the samples. The AFM is actually a Nanoscope which can go from micron scale to nanometers depending on the model and the operator (user). The AFM actually has contact with the sample by touching it. It is not an optical technique and the images are computer generated. Fig.3.5 depicts the schematics of the AFM working principle. The most simple description of the AFM is that the triangular needle scans all over the sample while the laser (usually red) shines on top of it. The needle tip is attached to the microsized spring that is called a cantilever.

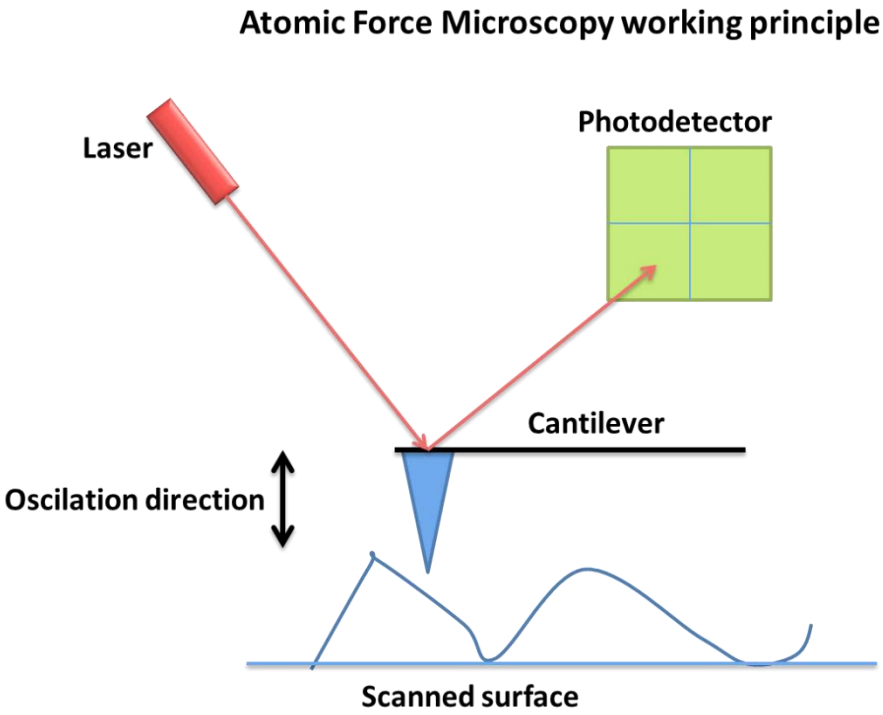

Figure.3.5 shows the schematics of the AFM microscope. The main part of the AFM is the head which is scanning the specimen. The tip (blue triangular in the image) is touching the surface of the specimen and the holding spring called a cantilever is bending. The laser is shining on the tip and the reflection angle of the laser is changing. The reflected laser is going to the photodetector which is connected to the analyzing computer.

When the tip is scanning the surface the cantilever is bending and the tip is moving upwards and downwards changing its height. The height changes in a few nanometers and the laser that falls on the tip is reflected to the detector. Everytime the height is changes the reflection of the laser spot changes the position on the photodetector. So during one scan we have only one line of pixels. To scan the whole area usually the AFM table is moving to x and y axis. To scan the area of 10X10 micrometers of a sample with the AFM model D3100 we typically need around 30mins. This would also

depend on the parameters adjusted. The scanning speed should be 0.4Hz. The surface of the sample can be almost anything from soft materials like polymers to nanodiamonds. The rougher the surface is the easier it is to brake the tip. Typically mica or silicon wafer surfaces are suitable for the AFM samples. The samples can be prepared by drop-casting the material on top of the substrate which leads to the rough surface in most of the cases. Or it can be spin-coated which leads to thin and smoots films.

3.8.2 AFM Tapping Mode

The AFM has two main modes. The contact mode and the tapping mode. It is very important to mention the difference between these two modes. In the contact mode described in the previous subchapter we have a contact between the tip and the surface of the sample. In the contact mode the tip is dragged all over the sample. But it also has some disadvantages. In the contact mode the tip dust and dragcitaverch ñ the sample thus preventing accurate results. Also the probability of breaking the tip in the contact mode is higher. This is where the tapping mode comes to an aid. In the tapping mode everything happens the same as in the contact mode but with one difference. In the tapping mode or as it is sometimes called the intermittent-contact mode the tip oscilates. The spring jumps up and down fig.3.5 It constantly oscilates and touches the surface of the sample at the lowest point of oscilation.

3.8.3 Scanning with Tapping M ode

In the tapping mode the tip would do exactly the same as in the contact mode it will touch the surface (only once) the cantilever will bend according to the sample surface roughness. But the probability of catching dust or any other molecule is much decreased and also breaking it is not very probable anymore. Therefore extending the life of the probe (cantilever and the tip).

3.9 UV-vis and Photoluminescence S pectroscopy

The UV-Vis and photoluminescence spectra of the CdS nanoparticles in the PPI[G4] solution were recorded at room temperature using a Cary 50 UV-Vis spectrophotometer and a Cary Eclipse fluorescence spectrometer (both Varian Inc.), respectively. The monochromator slit width was 10 nm.

3.9.1 UV-vis Working P rinciple

The UV-vis spectroscopy is the ultraviolet-visible range spectroscopy. It is considered as the most simple spectroscopic optical technique. The UV-vis spectrometer schematics are shown in Fig.3.6. The UV-vis has a light source (usually two lamps: UV and the visible range). The light source is a powerful lamp that shines trough the slit (called the entrance slit) then it goes to the diffraction grating or prism. Then the visible light is dispersed into different wavelengths and enters the second slit called the exit slit. From the exit slit it hits the sample which can be from a solution to a thin film. After it hits the sample a portion of light is absorbed by the sample material. After the absorption it reaches the detector which then tells us what energy portion was absorbed and the intensity of the light beam. From that it calculates the intensity of absorbed light by a sample. After the light dispersion from the prism we see a light dispersion or a rainbow. To avoid all the colors hitting the sample we need the exit slit which is a small hole designed to let only one wavelength to pass. In the UV-vis spectrum graph there are x and y axes. The axis y stands for intensity which depends on the photons passed through the sample. And the x axis represents the wavelengths of light. To achieve different wavelenghts of light during the scan the prism in the spectrometer slowly moves and allows different wavelengths of light to passs through the exit slit.

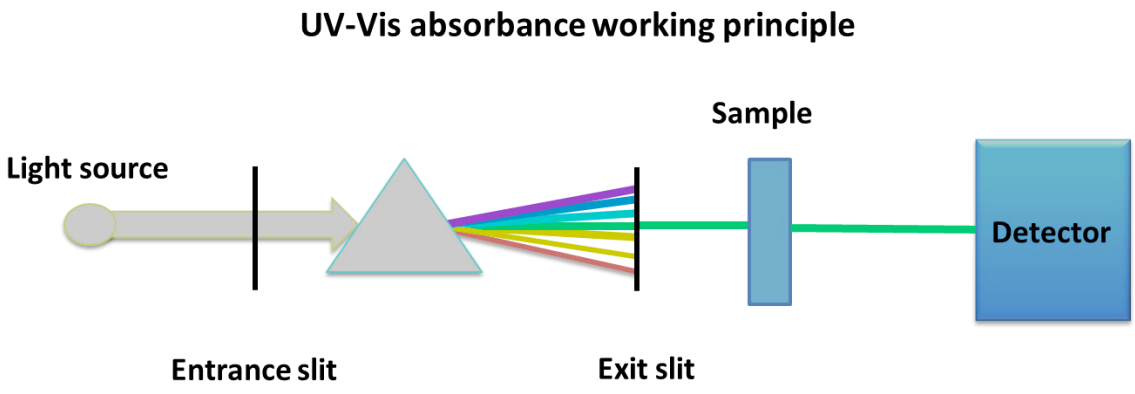

Figure.3.6 shows the UV-vis chematics. The light source goes throught the slit and then through the prism which breaks the light into many wavelengths. Then the exit slit allows one wavelength to pass which goes through the sample and then to the detector.

3.9.2 Photoluminescence Working Principle

The Photoluminescence spectroscopy is one of the most widely used spectroscopies in optics for semiconductors and a variety of materials including organics. The schematic depiction of PL spectroscope is in Fig.3.7. PL consists of a light source which is exciting the sample. The sample emmits back another photon of a lower wavelength and hits the detector. The role of the monochromators here is to are re-diffraction and spherical aberrations. Monochromators basically increase the resolution making it more precise and easier to analyse.

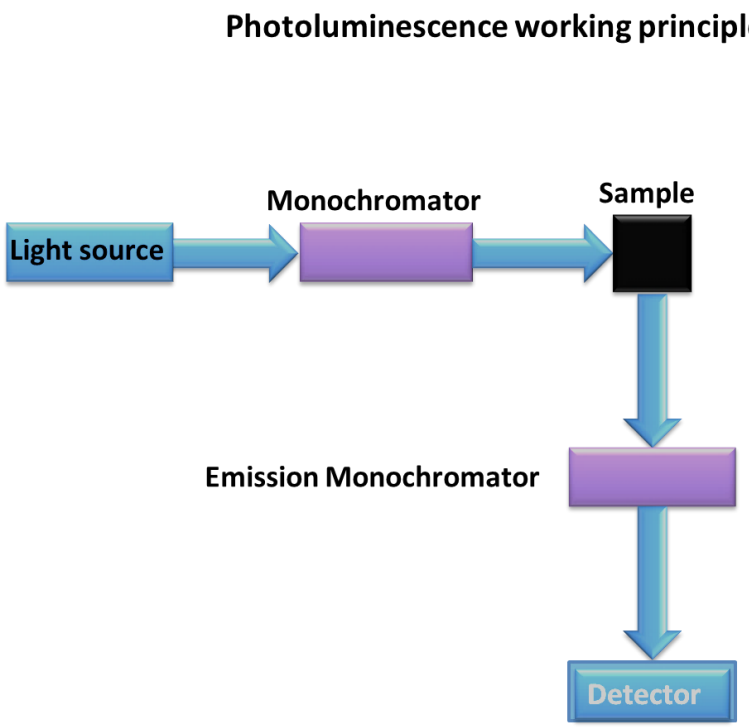

Figure 3.7 depics the working principle of the photoluminescence spectrometer. First the light source shines on the monochromator which then gives one wavelength to excite the sample. After the light hits the sample another wavelength is emitted already by a sample. After it is emmited by a sample it reaches the emission monochromator and then the detector.

3.9.3 PL Signal from the Material

When the photon hits the target it gets absorbed by an electron. Then the electron gets excited and goes to the higher energetical state. However, the excited electron does not stay long in the excited state and jumps to the lower energetical state emmiting the photon. The emitted photon is the photon that is absorbed by a detector in the PL spectroscope which makes the PL spectra.

3.10 Nuclear Magnetic Resonance

The Proton NMR analysis was performed in deuterated chloroform at 300MHz. NMR is a powerful and common technique in organic chemistry [194] and physics [195]. The NMR consists of a magnet that is capable of producing a uniform magnetic field and sources of radiofrequency. Magnets are usually superconducting and are cooled to very low temperatures like 4K (Kelvin). To achieve this temperature liquid helium is used. Modern instruments are capable of producing magnetic fields of 10T (Tesla) Fig.3.8. The NMR is for magnetic field interaction with the nuclei and not with electrons. A nucleus has magnetic moments that interact with the applied magnetic field. The magnetic moment of a nucleus may differ from the applied magnetic field and the electronic orbital angular momentum may be induced (circulation of electronic currents) and gives a rise to a small additional magnetic field at the nuclei. So when the external magnetic field 'hits' the nuclei it affects the nuclei local magnetic field and every nuclei has a different electronic structure near it. So every nuclei has a specific signal response (which also depends on the environment of the nuclei).

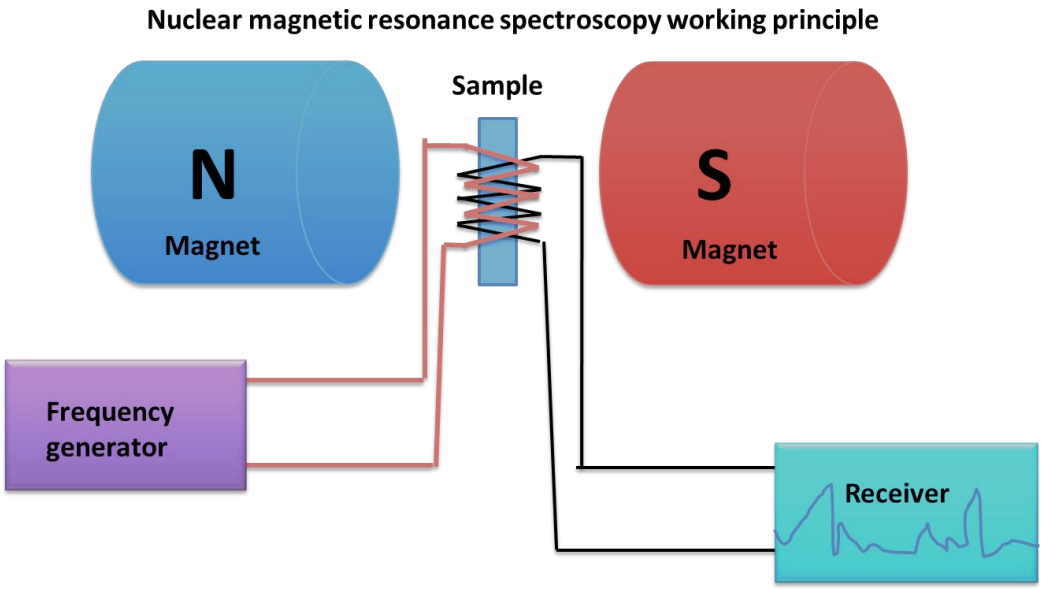

Figure 3.8 depicts a schematic diagram of the NMR spectrometer. The magnets create a large field of up to 10T. The sample is in the magnetic field. Radio frequency is generated by a frequency generator and the wires coil the sample. The second coil is receiving the signal which is then received by a receiver and analysed.

3.11 Data Analysis

The data from the spectrometers was analyzed using Origin pro. software. And the files from the AFM were analyzed using Gwyddion software. The size distribution of the nanoparticles was made using Gwyddion first. The desired TEM or SEM image was chosen first. Then objects were marked on the image and the data collected from the Gwyddion. Then it was imported to Origin pro and the graphs of size distribution were drawn.

3.11.1 RGB Light Coding

The coding of light was one of the most important parts in the light-induced synthesis. The RGB light code is the automatic sequence which includes 1 second for every wavelength (Red, Green, Blue and white then repeating the sequence again). To better explain the coding we need to see the graphs depicting the constant wavelengths and the interrupting wavelengths of light Fig.3.9.

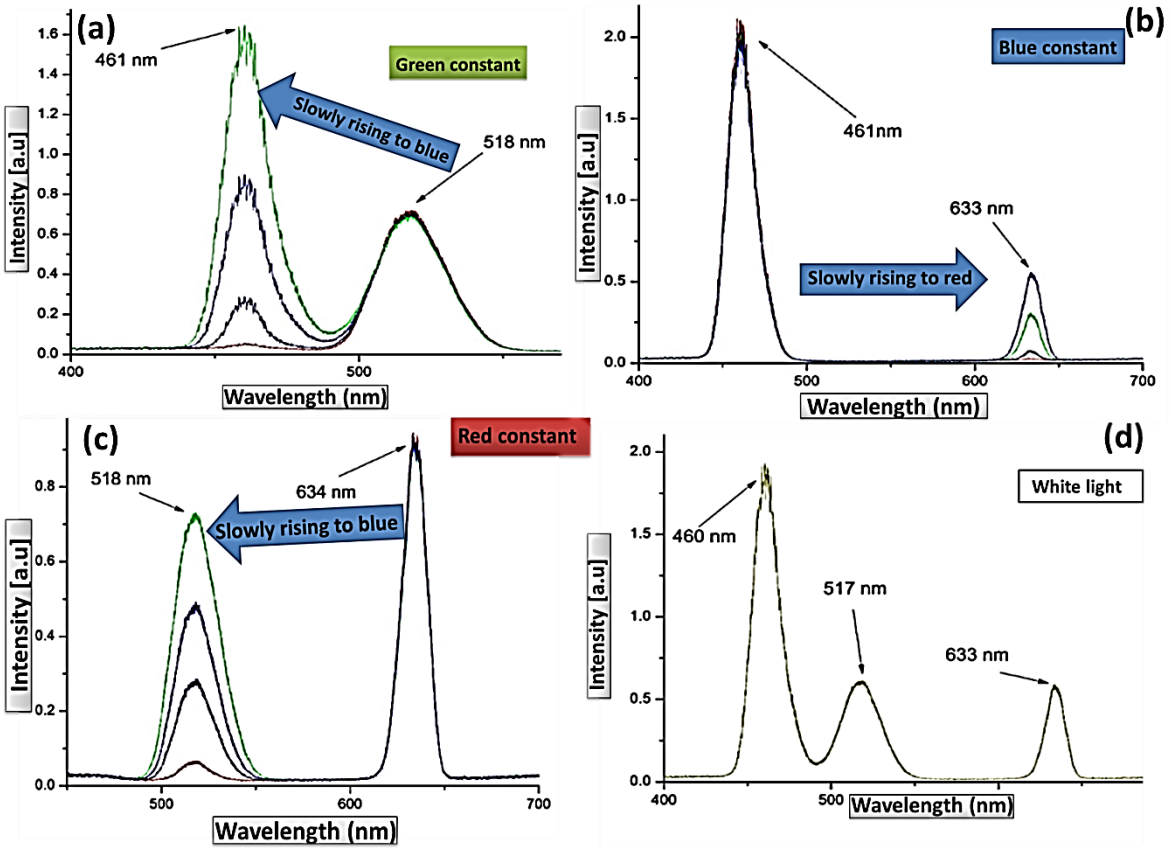

Figure 3.9 shows the LED spectra during the RGB code. (a) Green constant then rising to Blue constant (b) and then to Red constant (c) after rising to blue but then switches all the wavelengths and we have a white light (d).

Fig.3.9 requires special explanation. When the RGB code starts we have a Green LED on (called constant) after that slowly overlapped by the blue LED Fig.3.9 (a). The overlapping is relatively slow (1sec) by increasing the intensity of the particular wavelength. If we have a Green LED as a constant then the blue LED increases its intensity which overlaps with the green LED and at a certain time interval we actually have 2 wavelengths shining on the sample. After the blue LED reaches its intensity peak the green LED is off and another LED starts overlapping the blue LED. Fig.3.9 (b) the blue LED is constant (not changing) and the red LED is on the rise. The Red LED increases in intensity and after some moments we have the blue and red LED shining at the same time. When the Red LED reaches its intensity peak the blue LED is off.

3.11.2 Reaching White LED Peak

After reaching red the LED light is a constant and the blue LED increases in intensity Fig.3.9 (c). However, this time the blue LED will not reach its peak alone and the red LED will not get off. At one point all the wavelengths of light switch on with their highest intensities overlapping each other and we will have the white light LED Fig.3.9 (d). After a second the whole process will repeat itself over and over again.

Chapter 4 Study of Polymer Film Morphology Tailored by Solvents and LED

In this chapter the results of the experiments conducted with polymers will be analysed in detail. Polymer morphology change was induced in the polymer films using two methods: one using solvent mixtures and the other involving light.

4.1 P3HT-PCBMSolvent Effects on Nanostructura tion

This experiment was conducted using P3HT and $PC_{[70]}BM$. These two materials were mixed and dissolved in various solvents. Also the materials were dissolved separately in order to better investigate the effects on the nanomorphology of every solvent. The solvents were non-polar such as hexane, cyclohexane, toluene, chloroform (CF) and four polar aprotic solvents as chlorobenzene (CB), tetrahydrofuran (THF), dimethylformamide (DMF). For a proper investigation of the influence on the polymer morphology a step by step designed experiment with at least one polymer type is required. Since one the most popular semiconducting polymers is P3HT as a donor and $PC_{[70]}BM$ as an acceptor the further experimental investigation was conducted using only them. The light induced nanostructuration showed unexpected results and the P3HT/$PC_{[70]}BM$ system was not enough for a proper analysis. The observed effect was also checked with another polymer PTB7 in the PTB7/$PC_{[70]}BM$ system with the same conditions as P3HT/$PC_{[70]}BM$. The set of the same experiments was carried out in order to make a comparison and draw optimal conclusions. The colour set in every AFM analysis was chosen to best highlight the features of the polymer film and the most important image details. Fig.4.1 AFM image of P3HT/$PC_{[70]}BM$ in chloroform. The Fig.4.1 will serve as a reference since it has only one solvent and was not affected by external fields. As some works suggest the P3HT morphology depends on packing [196] and also on temperature [197]. This is why the polymer nanostructuration experiments were conducted at room temperature.

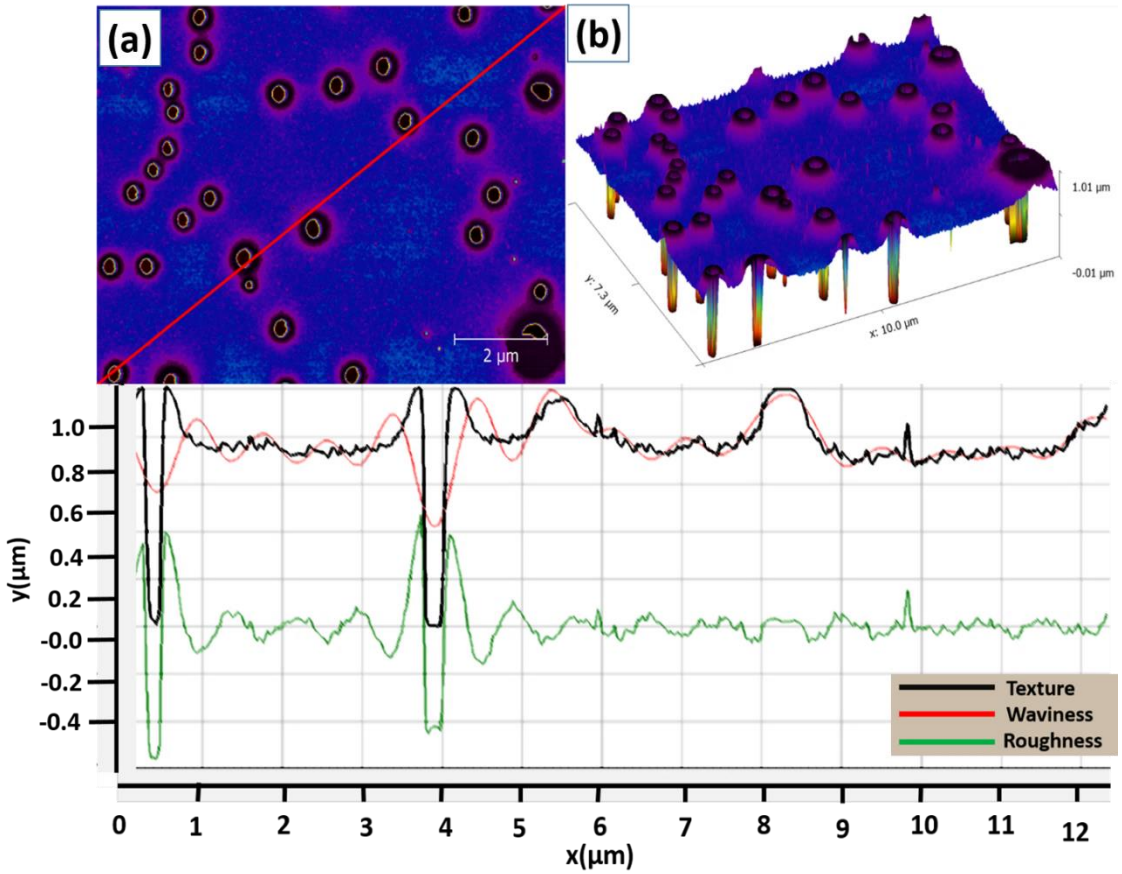

Figure.4.1 The AFM image of the P3HT/PC$_{[70]}$BM in chloroform. (a) shows volcano-like structures with few hundred distributed over the sample in particular manner as if they attract each oth family. (b) shows a 3D model of the (a). As it can be seen top and expand at the bottom. The graph below is the roughness of the film from (a) red line. The black line in the graph corresponds to texture; the red corresponds to waviness and the green to roughness.

As it is shown in Fig.4.1 the morphology of the P3HT/PC$_{[70]}$BM looks ñvolcano and the 3D image confirms the similarity of these structures to actual volcanos. However, the most surprising feature is the distribution of the holes over the sample. The AFM scans showed that the ñvolcanosò statement means that there is a reason why we get nanofeatures in a particular arrangement. The distance between the holes can either be interpreted as an arrangement that occurs in either rows, of two or stribution can be related to any of the system components i.e. to P3HT or PC$_{[70]}$BM or/and due to the solvent which is chloroform in this case. As we will see later the final morphology is influenced by all components (P3TH, PCBM and the solvent). The next AFM scan was PCBM in chloroform alone Fig. 4.2.

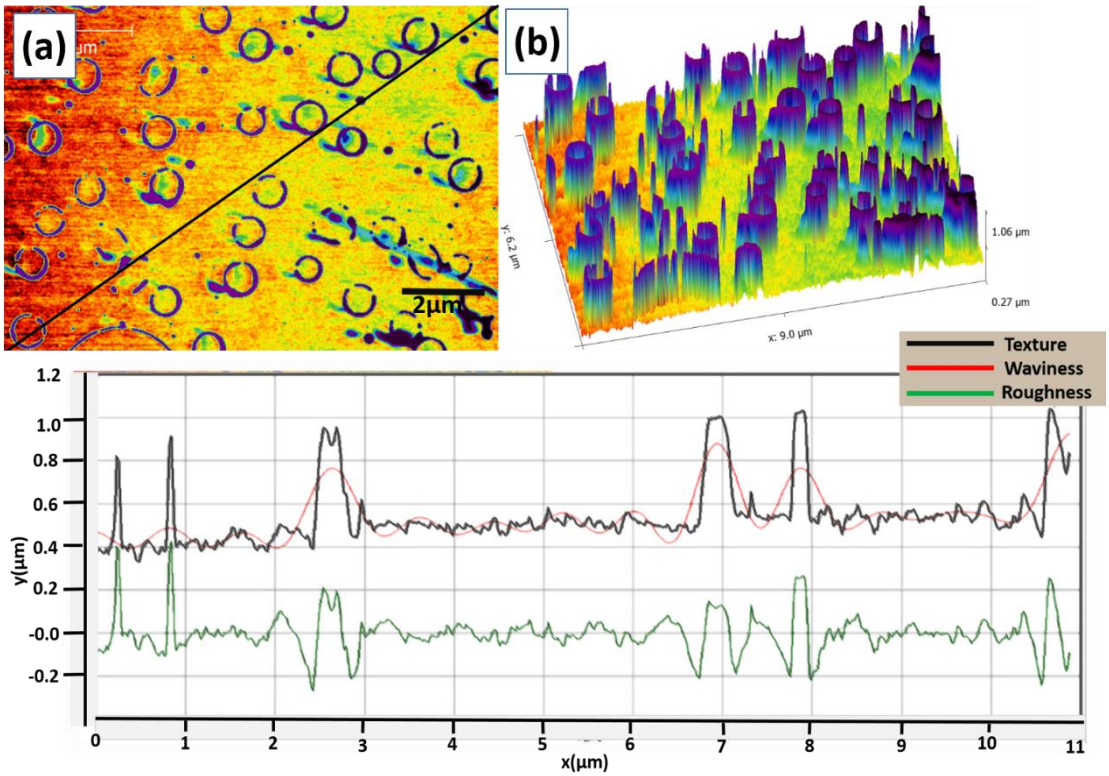

Figure. 4.2 The AFM image of the $PC_{[70]}BM$ in chloroform. (a) shows AFM top view. As it can be seen the circles are not complete (most of them) look but a moòt añnvyonhocre. The graph below in the roug The black line in the graph corresponds to texture, the red corresponds to waviness and the green for roughness.

Fig.4.2 depicts the $PC_{[70]}BM$ in chloroform. This micrograph confirms the appearance of ñvolcanosò is the P3HT. However, the structures in Fig.4.2 d not are not exactly the same as in Fig.4.1. This is due to the P3HT as well. The P3HT has also an influence in morphological formations. For better understanding of the influence of PCBM we need to understand the influence of solvents over the PCBM alone. Another sample was prepared with the $PC_{[70]}BM$ alone in hexane. Dissolving in hexane was difficult and required an ultrasonic bath for 10-15minutes. The morphology was more micro-sized rather than nanosized Fig.4.3.

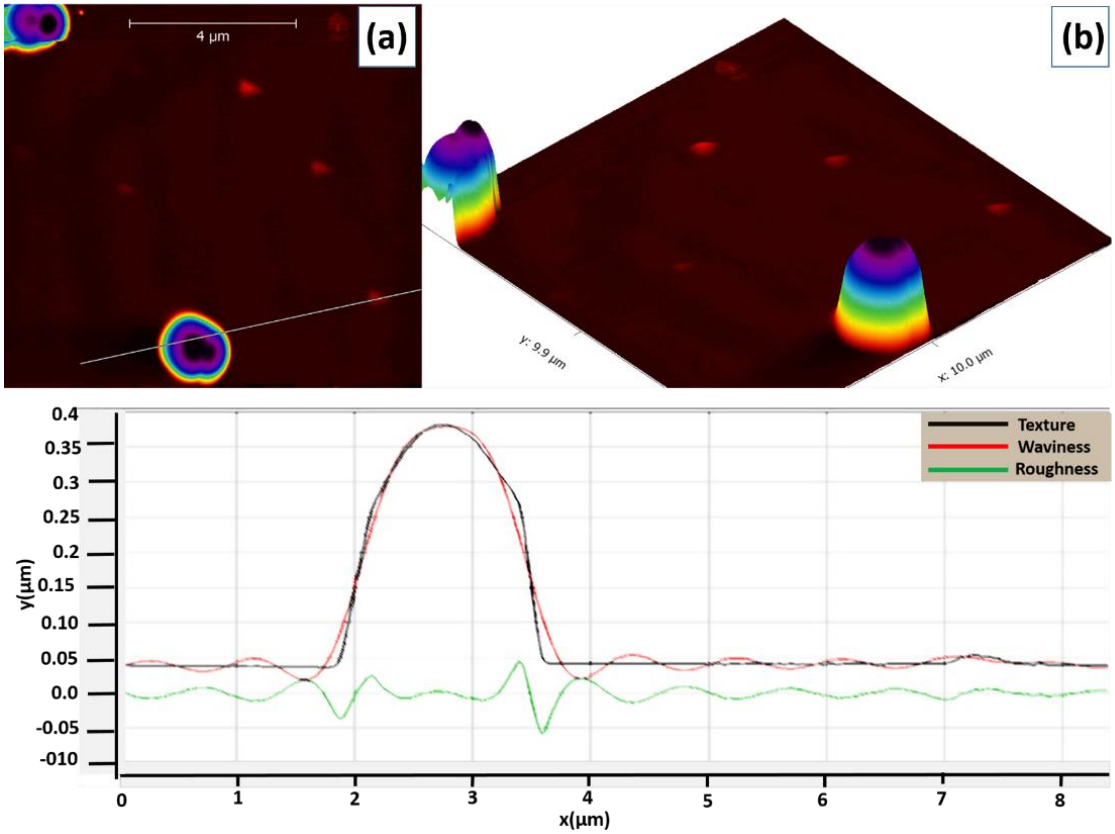

Figure.4.3 The AFM images of the $PC_{[70]}BM$ in hexane. (a) the PCBM ñclumpsò show micrometers in width and distributed over the sample with great distances of tens of microns. (b) the 3D model showing no ñvolcanoò formations. The black li texture; the red corresponds to waviness and the green to roughness.

The PCBM clumps were distributed over the sample but with huge inter feature distances of 20 and more micrometres. Additionally, the or ñtubeò shaped as in Fig.4.2 and Fig.4 ñballsò or ñeggsò an shaped and do not contain perfect or holes. Fig.4.3 suggests a significant influence of the solvent since we do not observe ñvolcanosò any more a different solvent does not provide sufficient information or proof. To prove the influence of the solvent another AFM scan was performed using the $PC_{[70]}BM$ in THF. This AFM scan shown in Fig.4.4 indicates structures that visually look similar to the Fig.4.3 with some important differences.

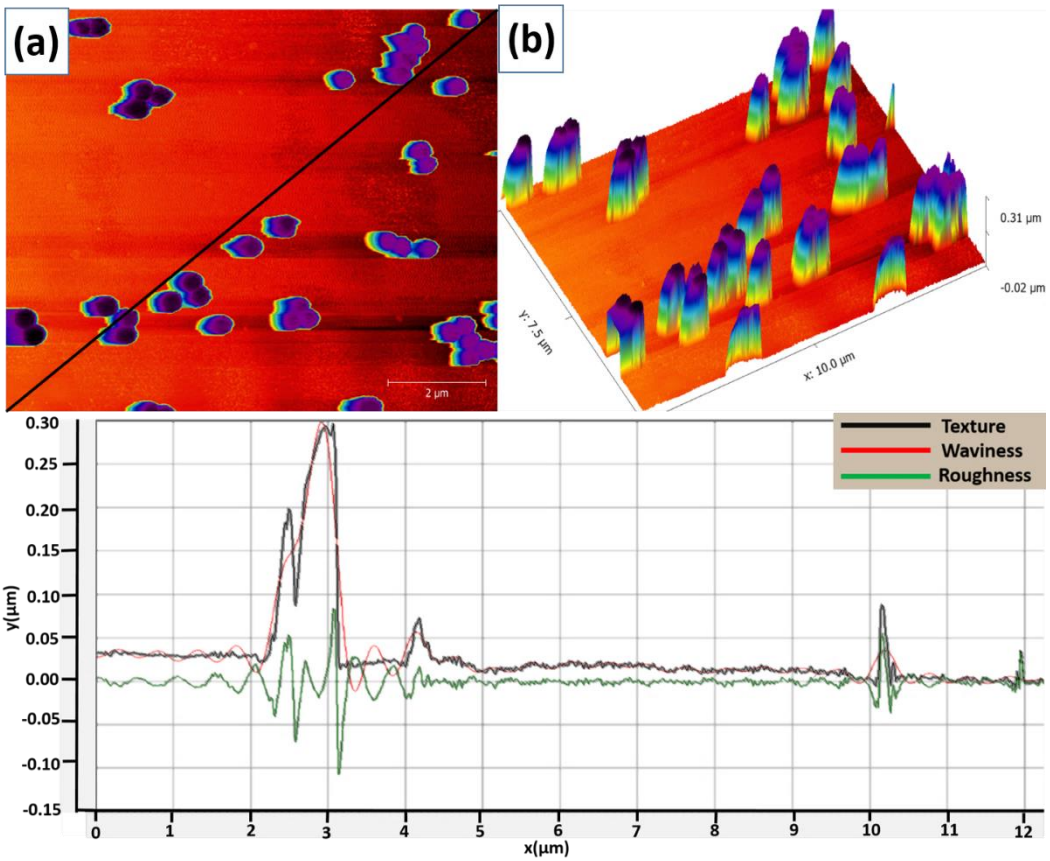

Figure.4.4 The AFM images of the PC[70]BM in THF. In (a) we can see rou a particular manner usually two to three and more. Also s shows 3D model in which we can see the formation of the PCBM ñhillsò that are v and similar. The black line in the graph corresponds to texture, the red corresponds to waviness and the green for roughness.

The main difference is the size of the structures and importantly the deposition over the sample. In the case of the THF as a solvent the PCBM structures behave very similar to the one used with the chloroform. However, in the case with the THF they do not form ñvolcanosò or ñtubesò and hav could be compared to the Fig.4.3 vit seems that the THF inforces assemble PCBM ñhillsò cmloorsedonyñ-caiork eò fodrinstarib These ñcoloniesò were distributed over manner. Which was later shown to be due to the distribution changes when combined with some other solvent and mixing the P3HT with the PC[70]BM. The scan with the DMF was performed and no ñcolonyò or ñvol observed Fig.4.5.

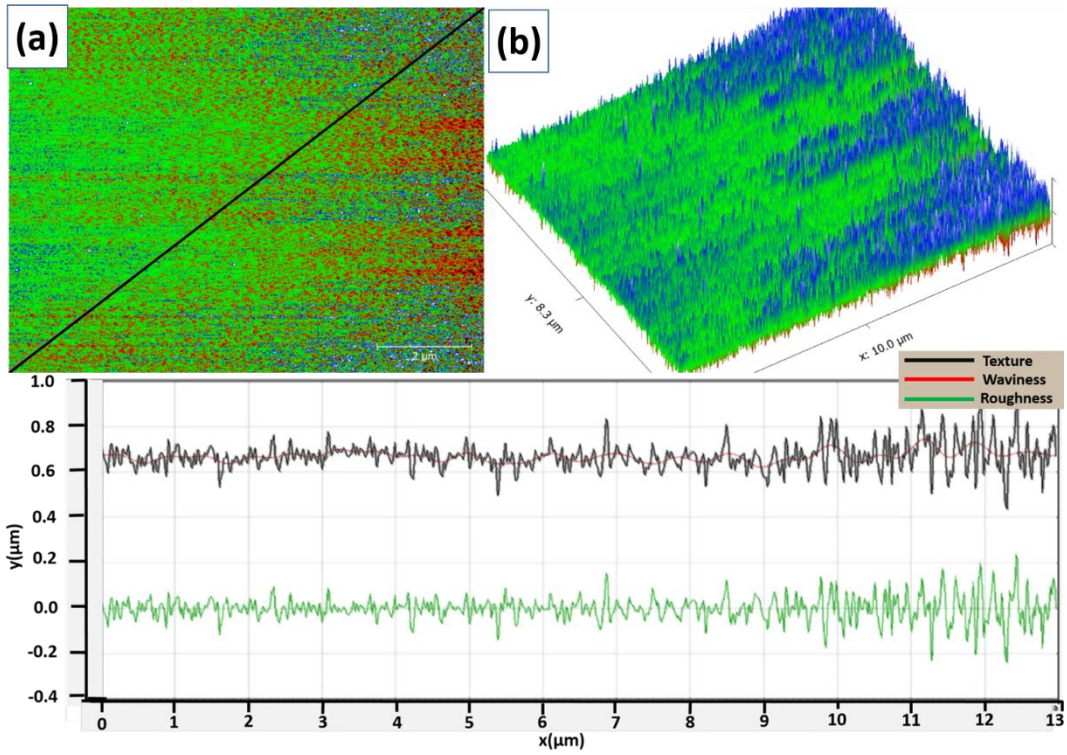

Figure.4.5 depicts the AFM images of the PC$_{[70]}$BM in the DMF. (a) difficult to define the features. However, the color was chosen for a maximum highlight of the features. (b) the 3D model shows the roughness which is almost dotted and distributed without a ñ c o l o n y ò m a n n e r o v e r t The black line in the graph corresponds to texture, the red corresponds to waviness and the green for roughness.

This scan in Fig.4.5 confirms the influence of a solvent over the PCBM molecule distribution. The AFM image in Fig.4.5 looks more like vertical needles and the scan was performed a couple of times changing the AFM tips in order to eliminate any scan errors. For now, it is too early to make conclusions and try to link the morphology with the solvent parameters such as dielectric constant or dipole moment. The objects in Fig.4.5 are very small and have no particle like similarities like those observed in previous scans (Fig.4.1 to Fig.4.3). In Fig.4.5 (b) the 3D image shows blue lines that are vertical and are highest and the green lines that are diminishing. Another sample of PCBM in chlorobenzene was prepared and characterized using the same technique and method (same speed spin-coating) Fig.4.6. This time the film surface is different from the previous scans and it is similar to the one in Fig.4.5. The PCBM do not form l a r g e c l u m p s n e i t h e r ñ v o l-like formations spread ñ t u b over the whole sample. This investigation shows the influence of different solvents over the same material which is PCBM in this case.

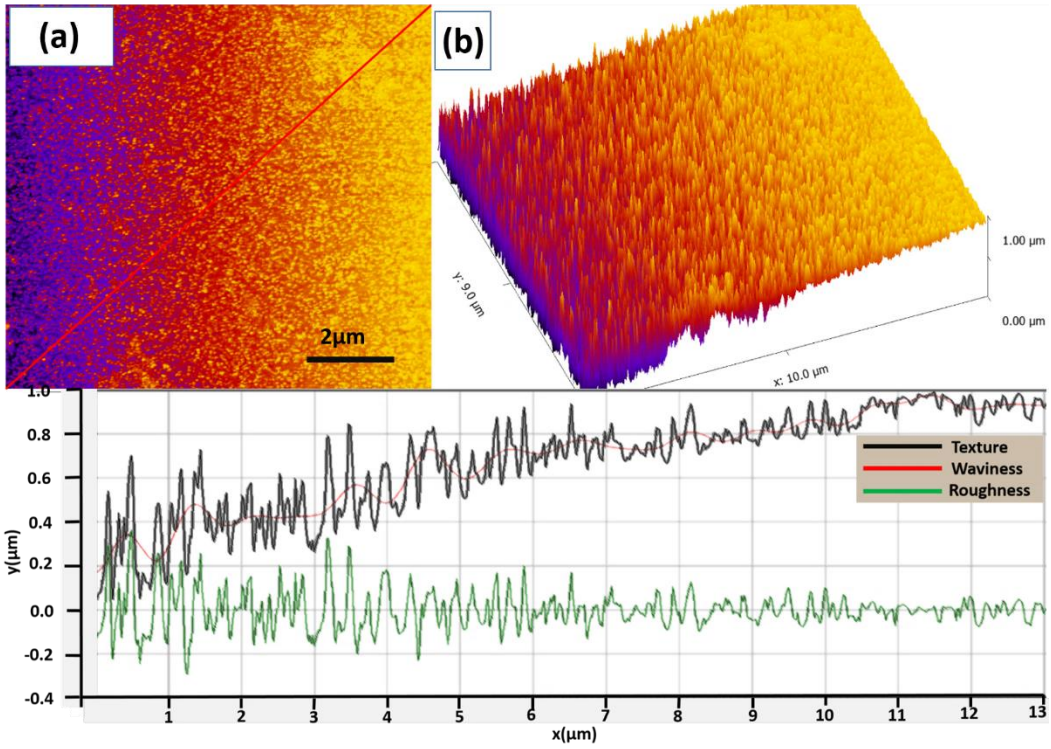

Figure.4.6 The AFM image of the PCBM in Chlorobenzene. (a) has very small features but they have a higher distribution level and are deposited uniformly without leaving empty space on the sample. (b) the 3D image confirming the vertical PCBM distribution over the sample with decreasing roughness as confirmed by the graph below. The black line in the graph corresponds to texture, the red corresponds to waviness and the green to roughness.

The present AFM topography of the $PC_{[70]}BM$ in chlorobenzene might be attributed to the crystallization degree as was reported using the P3HT/PCBM [198]. Also it was reported that the morphology of the films depends on the concentration [198]. DMF and chlorobenzene are polar solvents and they have huge differences in dielectric constant values. However, the morphology does not look very different which means that the dielectric constant does not have an influence in the process of the morphology formation. Another parameter such as the dipole moment is 3.82 for DMF and 1.54 for chlorobenzene. The difference between these constants is 2.28. On the other hand, it is best to neglect these parameters and check the morphology using other solvents such as cyclohexane which has dipole moment equal to 0.0. Fig.4.7 Shows AFM image of PCBM in cyclohexane. Cyclohexane is non-polar solvent and has dipolar moment of 0.0. Dielectric constant is 2.02. The observed morphology in Fig.4.7 shows the formations that also do not look like ñ v a h o s ò o r ñ t u b e s ñ h i h l o l w s e ò v . e r T h i s A F M m i c r o g r a p h (F i g . 4 . 7) s h o w s u n i f uniform heights Fig.4.7 (b) and a graph roughness analysis. This result gives hints to what may be the most important parameters in morphology formation.

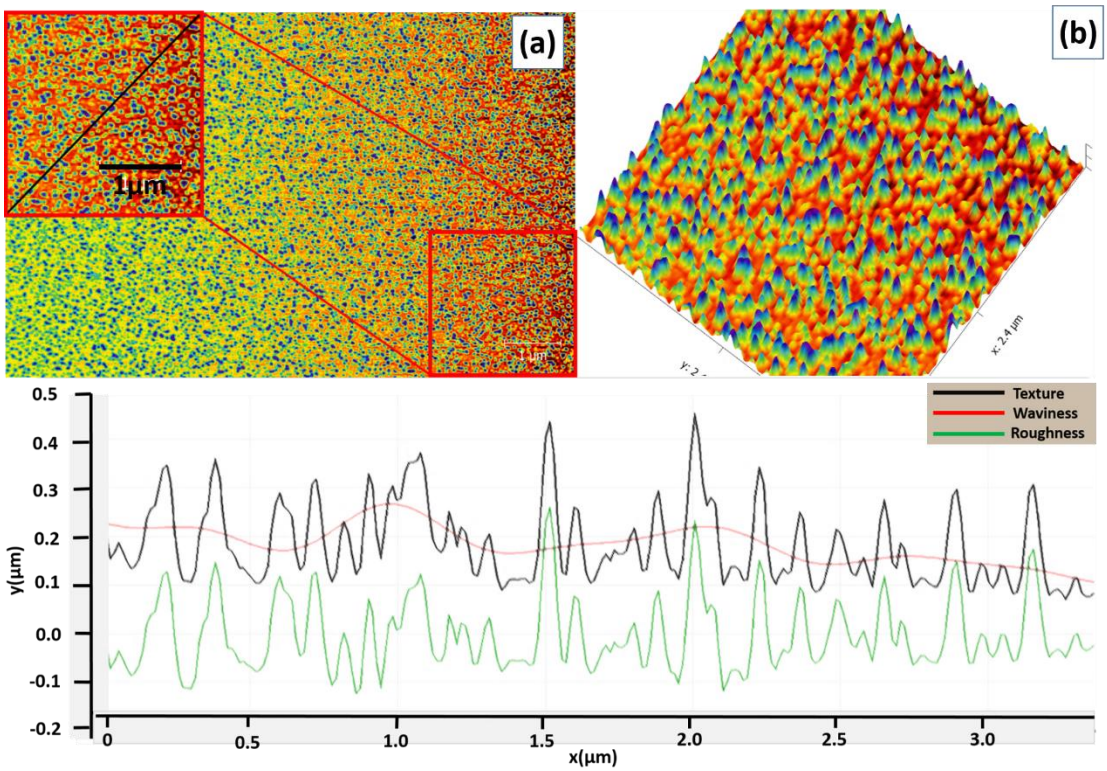

Figure.4.7 The AFM image of the $PC_{[70]}BM$ dissolved in cyclohexane. (a) shows that structures are formed uniformly over the whole sample. The red square was analyzed in detail in order to make a more precise analysis of the morphology. (b) the 3D model of the scan confirming relatively high width and height uniformity. The black line in the graph corresponds to texture, the red corresponds to waviness and the green to roughness.

It is clear that the greatest influence is due to the solvent (we are using the same concentration in all the samples 1mg/ml). On the other hand, the PCBM alone repeats very similar morphologies alone Fig.4.2. These effects could be due to the ranging solubility in different solvents. As it was demonstrated the morphological changes are caused by both the P3HT and the PCBM. However, the PCBM was investigated alone and with different solvents. The solvent influence over the PCBM morphology was demonstrated. While the P3HT/PCBM in chloroform and the PCBM alone in chloroform film morphologies look similar PCBM alone in chlorobenzene morphology is far from the reference Fig.4.1. This could be due to the solvent parameters such as the dipole moment.

4.2 Influence of Solvents and Solvent M ixtures on the P3HT/PCBM Morphology

For a proper investigation of the polymer morphology and to achieve optimal results it is necessary to use a small polymer system composed of a maximum of two components. This is why the P3HT/PCBM system was chosen for the investigation. The P3HT/PCBM is the actual active material for the organic solar cell and it is most studied [184]. This is a valuable reason for choosing the P3HT/PCBM. Fig.4.8 depicts the AFM image of the P3HT/PCBM system dissolved in cyclohexane. As compared to Fig. 4.7 where PCBM alone was in cyclohexane we can observe the similarities in the morphology.

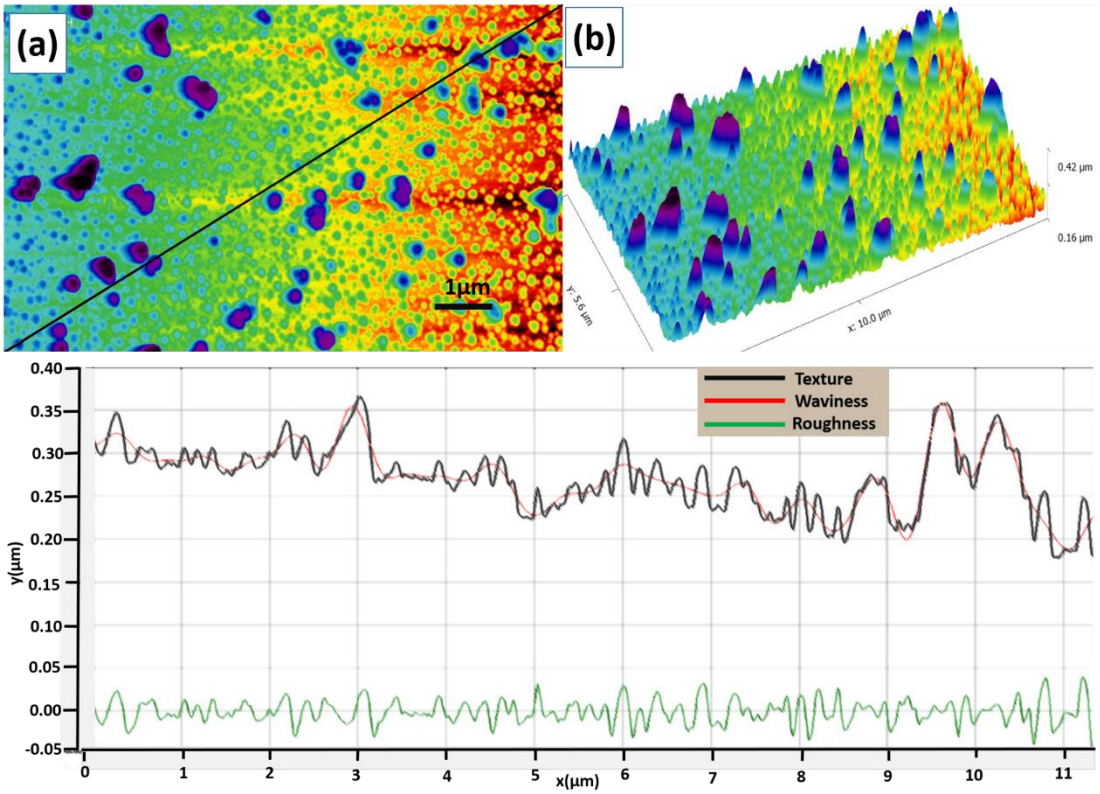

Figure.4.8 The AFM image of the P3HT/PC$_{[70]}$BM in cyclohexane. (a) shows large and small clumps over the sample. (b) wider fiolrmsati ans ahrs lower in diameter. The black line in the graph corresponds to texture, the red corresponds to waviness and the green to roughness.

These observations suggest that the PCBM is dominant in the formation of nanomorphologies with the P3HT. To prove the idea of the PCBM dominance we need to use another solvent which would not be as good as chloroform and not as bad

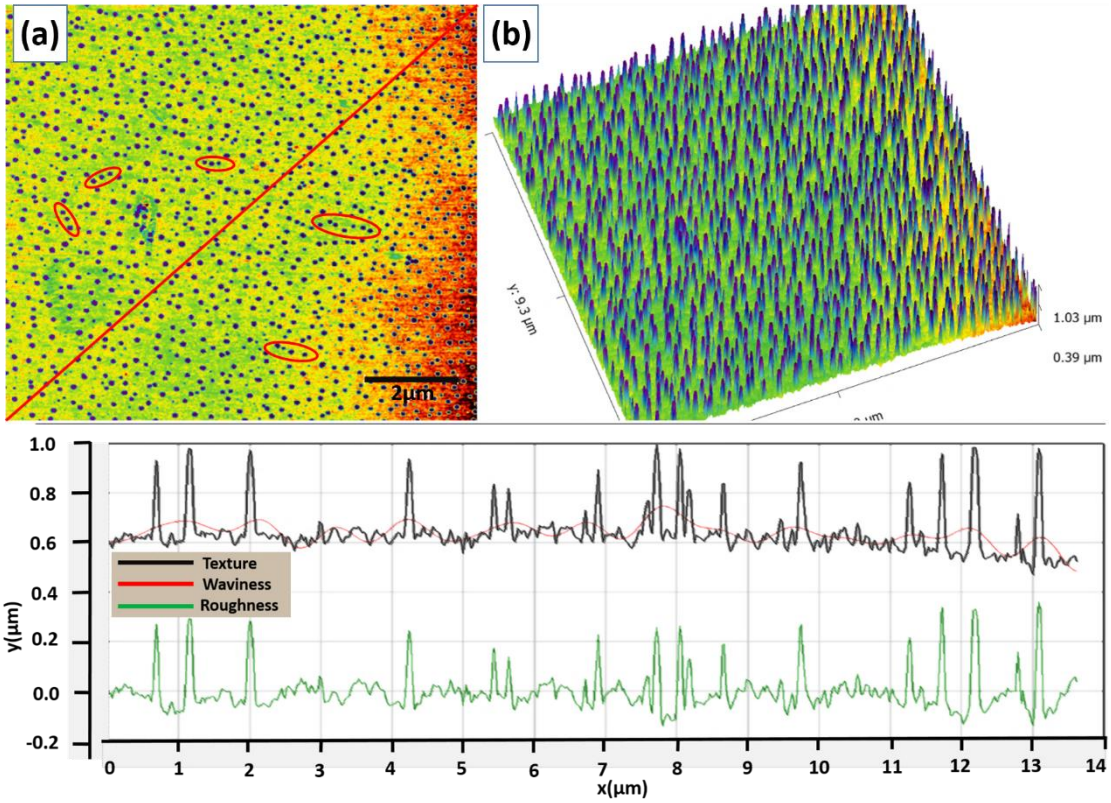

Figure.4.9 AFM image of the PC[70]BM in toluene. (a) Top view showing very uniform dots formed without any behaviour. (b) the 3D model showing vertical stic uniform height. The black line in the graph corresponds to texture, the red corresponds to waviness and the green for roughness.

as hexane or cyclohexane. Toluene is the perfect candidate. Fig.4.9 is the AFM image of the PCBM alone in toluene. As we can see t are distributed in groups Fig.4.1 (a) red circled. Toluene is a non-polar solvent that can dissolve both the P3HT and the PCBM. The dipole moment of toluene is 0.36 and the dielectric constant is 2.38 which is close to the values of cyclohexane and hexane (2.02 and 1.9 accordingly). However, hexane is a poor solvent for both the P3HT and the PCBM. Fig.4.10 shows the AFM micrograph the P3HT/PCBM in toluene. Fig.4.10 is comparable to that in Fig.4.9 where the PCBM in toluene alone. Fig.4.10 also has ñfamilesò or ñislandsò (Fig.4.10 (a) whit circled. This result sheds light on the role of the PCBM in the P3HT/PCBM morphology formation. And while some solvents do not cause the formation of ñislandsò (chlorobenzene or DMF) the toluene P3HT/PCBM and the PCBM systems.

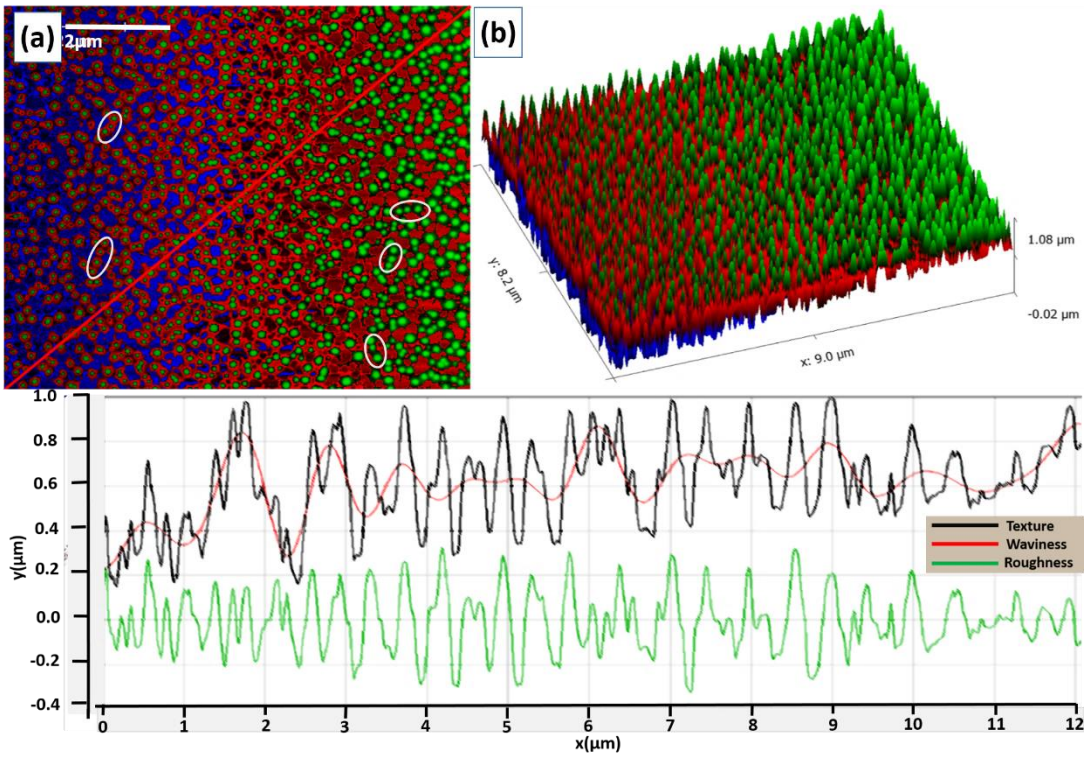

Figure.4.10 The AFM image of the P3HT/PC$_{[70]}$BM in toluene. (a) s h o w s r o u n d s h a p e that do not contain holes and are uniformly distributed over the sample. (b) the 3D model of the image. The black line in the graph corresponds to texture, the red corresponds to waviness and the green to roughness.

As demonstrated in the subsection 4.4 of the present work the nanomorphologies or morphologies of the P3HT/PCBM and the PCBM alone in different solvents vary. However, we can conclude that the PCBM itself has the main influence on the final morphology in the P3HT/PCBM system. For a better understanding of the possible control over the nanomorphology a more profound investigation is required. The next subsection 4.6 deals with the P3HT and the PCBM dissolved in different solvent mixtures.

4.3 Mixed Solvent Approach

This part deals with polymers used in previous sections (4.4 and 4.2) the P3HT and the PCBM dissolved in a mixture of solvents and also in varying amounts of solvents. The purpose of the present subsection is to demonstrate that morphological control can be achieved by mixing solvents together varying amounts of solvents. Fig.4.11 is the AFM image of the P3HT dissolved in the THF and mixed with the PCBM which was dissolved in the DMF. As we can see the morphology is similar to that in Fig.4.4.

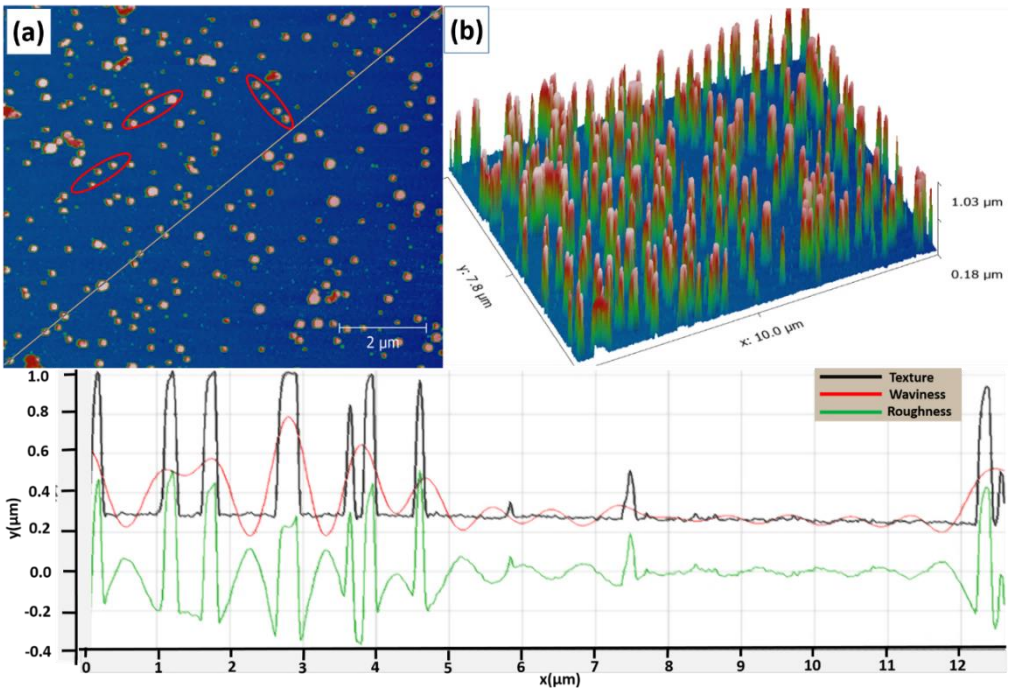

Figure.4.11 The AFM image of the P3HT 0.5mg/ml of THF and PC[70]BM 1mg/ml of DMF. (a) the ñislandsò are still present. Also the format image showing vertical ñislandsò. The roughness graph is t (green).

In Fig.4.4 the PCBM alone was dissolved in the THF. The observed morphology is very similar to that in Fig. 4.11 containing ñgroupsò of main difference is the diameter of the structures. In Fig.4.11 the diameter is smaller suggesting the influence of the P3HT. On the other hand, it is not enough to conclude the influence of the PCBM from Fig.4.11 without a comparison of the same system with an increased amount of PCBM. Fig.4.12 is the AFM image of the P3HT/PCBM dissolved in the THF and the DMF as in Fig.4.11 but with the PCBM amount increased two times. As we can see from Fig.4.12 the morphology obtained is basically the same as in Fig. 4.11. However, the amo tion of ve is different. In Fig. 4.12 the ñislandsò ñis ds ò. This result role s of the PCBM in the formation of nifica ñislandsò. If this statement is true, t decrease the amount of islands or completel is the AFM image of the P3HT/PCBM in the THF and the DMF but with decreased amount of the PCBM two times. The image clearly previously observed (Fig. 4.11 and 4.12). Th randomly distributed nanoparticles rather than polymer formations. Fig.4.13 also shows formations which look more like ag

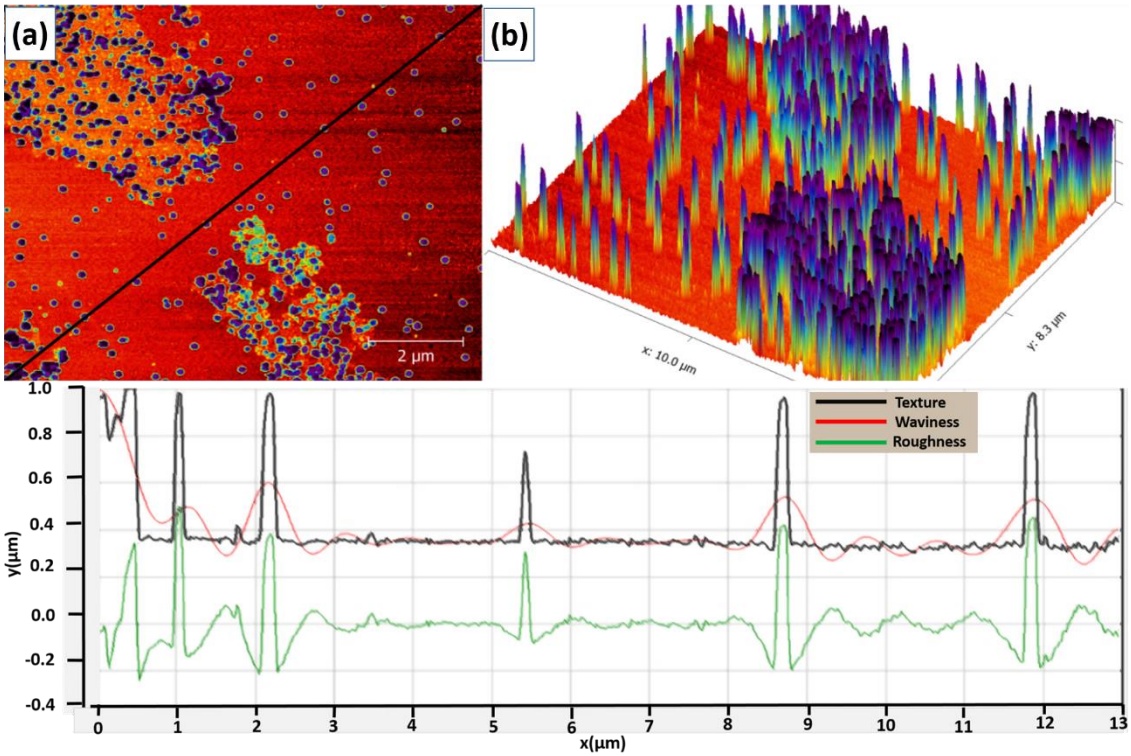

Figure.4.12 The AFM image of the P3HT 0.5mg/ml of the THF and the PC[70]BM 2mg/ml dissolved in DMF. (a) higher amount of ñ is l the 3D structure and ml y shows increase in vertical islands. The graph is the texture (black), waviness (red) and roughness (green).

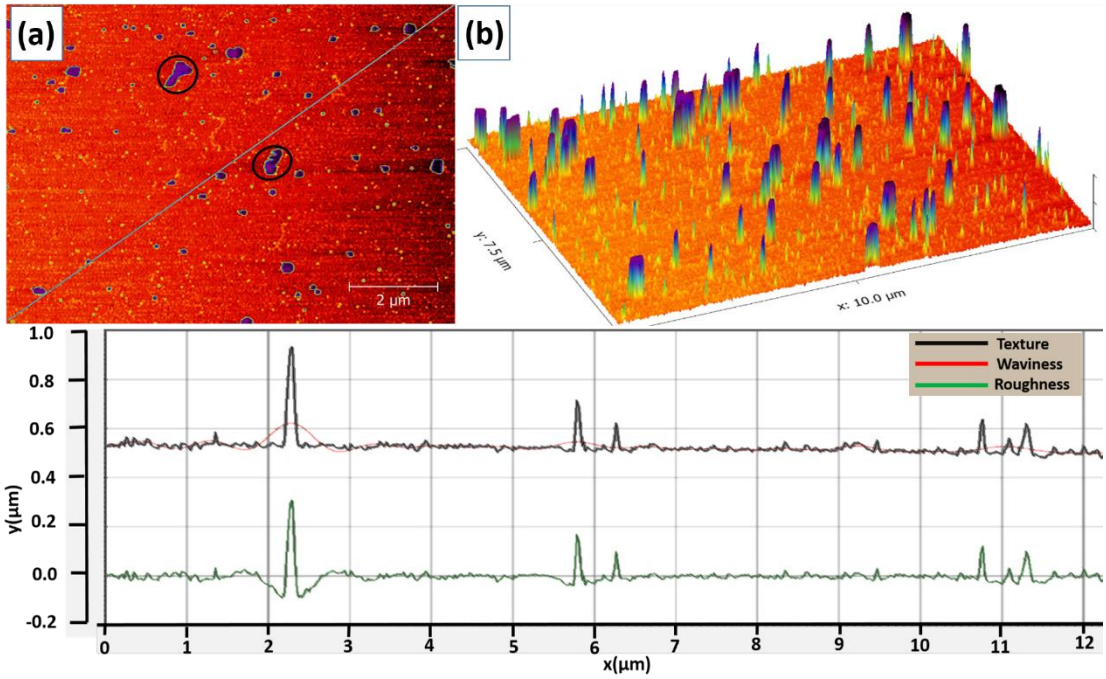

Figure.4.13 The AFM image of the P3HT 0.5mg/ml of the THF and the PC[70]BM 0.5mg/ml of DMF. (a) indicates clumps and ruins of the ñ is nanomorphology formation (black circled). (b) the 3D showing the height distribution of the vertical formations. The graph is the texture (black), waviness (red) and roughness (green).

This result undoubtedly confirms the influence of the PCBM in the formation of the nanomorphology. For the final confirmation the amount of PCBM was decreased to 0.29mg/ml and the amount of P3HT was left at 0.5mg/ml. Fig.4.14 AFM image which finally confirms that the PCBM plays a major role in the providing the control possibility by varying the amount of PCBM. Fig.4.14 do not show any observable formations at all. In fact, any distinguishable features.

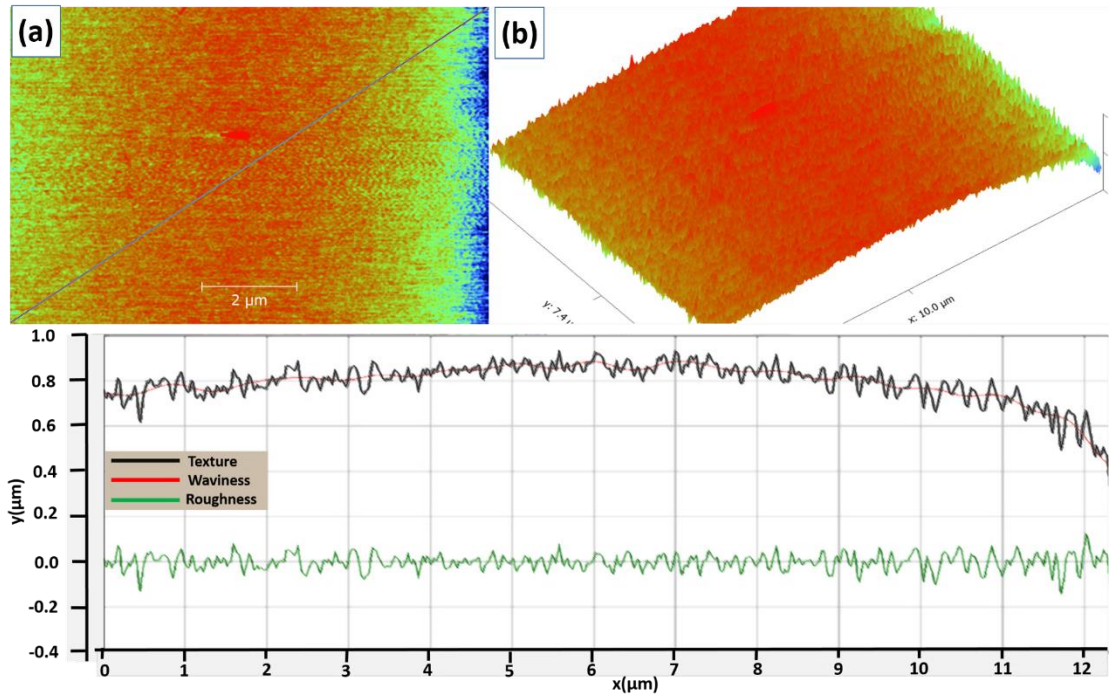

Figure.4.14 The AFM image of the P3HT 0.5mg/ml of the THF and the PC[70]BM 0.29mg/ml of the DMF. (a) completely ruined mixed and (b) formations or „hills". The graph is the texture (black), wa

The P3HT/PC[70]BM system morphology can be influenced by varying the amount of the PC[70]BM. While the amount of the P3HT does not show significant morphological changes PC[70]BM was proven to play a major role. These findings provide basic ideas on the control of nanomorphology in P3HT/PC[70]BM systems. Every solvent has a different molar mass and parameters such as capability to dissolve one or another polymer. Every solvent makes polymer molecules to be on a different distance from one another and also change the conformation. When the film from the polymer solution is cast onto the surface of the silicon or mica surface the polymer molecules

settle down in a particular manner which at the end forms the morphology. During the film formation the polymer chains might be arranged in various ways creating complex morphologies. The reason for different colours in every vial is the distance between the molecules which vary depending on the solvent Fig.4.15.

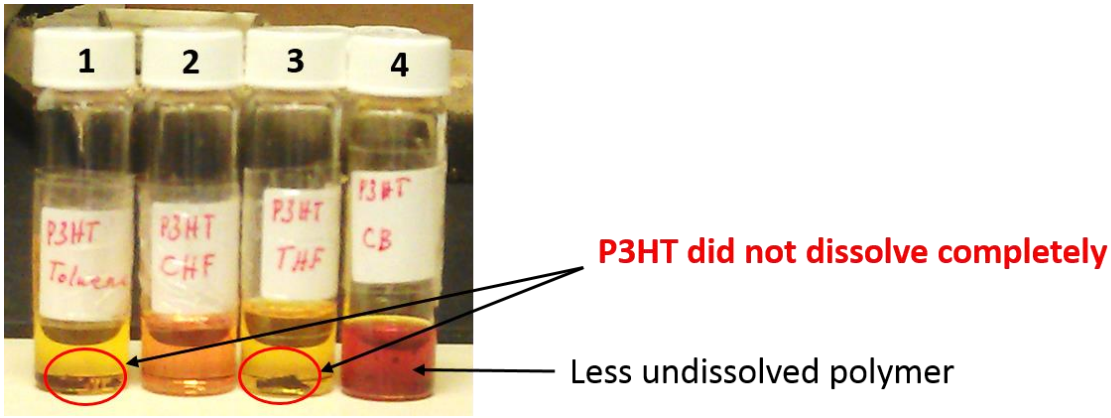

Figure.4.15 P3HT polymer dissolved in different solvents: 1 toluene, 2 chloroform, 3 tetrahydrofuran and 4 chlorobenzene. The concentration is 1mg/ml in all 4 vials.

4.4 PTB7/ $PC_{[70]}BM$ Light-Induced Morphology Control

In this subchapter the PTB7/PCBM nanomorphologies affected by light are discussed and analysed. The samples were exposed to blue and red LED light. Since shorter wavelengths have higher energy (blue light) and longer wavelengths lower energy (red light) it was the most logical choice for the sample irradiation. A mixture of PTB7/$PC_{[70]}BM$ was prepared in chloroform with concentrations 1mmol/ml under exposure of blue (461nm) and separately red (634nm) LED light. The LED exposure time was 12 hours. Non exposed sample was prepared in order to make a comparison. All the samples were deposited on a silicon wafer via spin-coating at 2500 rpm for 1 minute and characterized using the AFM D3100 in tapping mode. The difference in nanomorphology showed tendency depending on the wavelength of the light. Fig.4.16 AFM image of PTB7/$PC_{[70]}BM$ in the dark.

Figure 4.16 The AFM image of the PTB7/$PC_{[70]}BM$ 1:1 in chloroform reference sample: (a) Reference sample without the treatment of light. The voids are randomly deposited on the surface and the roughness is characterized on three lines and represented in (b). In the image (c) is zoomed red square from the image (a) and analysed in detail. The insert in the right corner shows height with specially chosen colour panel. (c) Shows roughness profile from (c).

The sample in Fig.4.16 was not exposed to any source of light and the vial was wrapped in aluminium foil to avoid daylight. As we can see in Fig.4.16 the AFM micrographs reveal the formation of voids or holes which range in diameter and are randomly distributed over the sample. Th
For more precise evaluation Fig.4.16 was analysed in detail. In Fig.4.17 the AFM image of PTB7/PCBM in chloroform (in dark) with a more detailed analysis of voids and 3D image. As it can be seen from Fig.4.17 the voids are ranging from 350 nm (void No.9) to 1.79 Õm (structures resembling volcanic) in d
structures rather than just nanoholes. The colours in the inset in Fig.4.16 (c) are made to better highlight the details. The same system showed an obvious change in void distribution and shape when exposed to the light. Fig.4.18 is the AFM image of the PTB7/PCBM exposed to the blue light for 12 hours. The structures change the shape to elongated distorted ellipse-like formations. Also a few round shaped voids were observed. The more detailed analysis in Fig.4.19 defined the roughness and void diameter (length).